

# HIGGS BOSON PRECISION STUDIES AT A LINEAR COLLIDER \*

Klaus Desch, University of Hamburg, Germany

## Abstract

This report summarizes the progress in the study of Higgs physics at a future linear electron positron collider at center-of-mass energies up to about 1000 GeV and high luminosity. After the publication of the TESLA Technical Design Report [1], an extended ECFA/DESY study on linear collider physics and detectors was performed. The paper summarizes the status of the studies with main emphasis on recent results obtained in the course of the workshop.

## OBJECTIVES OF THE STUDY

Elucidating the mechanism responsible for electro-weak symmetry breaking is one of the most important tasks of future collider based particle physics. Experimental and theoretical indications of a light Higgs boson make the precision study of the properties of Higgs bosons one of the major physics motivations of a linear collider (LC). Both the Higgs boson of the Standard Model (SM) and those of extended models will be copiously produced in  $e^+e^-$  collisions in various production mechanisms. A large variety of different decay modes can be observed with low backgrounds and high efficiency. These measurements allow us

to extract the fundamental parameters of the Higgs sector with high precision. The series of ECFA/DESY workshops aims at a comprehensive study of the physics case, a determination of the achievable precisions on Higgs observables as well as on a fruitful cross-talk between theory, physics simulations and detector layout.

A future linear collider offers also the option of photon-photon collisions from back-scattered laser light. The physics potential and progress in Higgs physics at a photon collider is discussed elsewhere in these proceedings [2].

## STANDARD MODEL HIGGS BOSON

### Theoretical Predictions

In  $e^+e^-$  collisions, the SM Higgs boson is predominantly produced through the Higgs-strahlung process,  $e^+e^- \rightarrow H^0 Z$  [3] and through the vector boson fusion processes  $e^+e^- \rightarrow \nu_e \bar{\nu}_e (e^+e^-) H^0$  [4]. The SM production cross-sections are precisely known including full electro-weak corrections at the one-loop level. For a recent review of the theoretical calculations see e.g. [5]. Recently the full one-loop corrections to the WW-fusion process have been calculated [6, 7]. The radiatively corrected cross-sections for Higgs-strahlung and WW-fusion are shown in Fig. 1. For Higgs-strahlung the corrections are positive for small Higgs masses and negative for large Higgs masses and are of  $\mathcal{O}(10\%)$ . For WW-fusion the corrections are of similar size but always negative.

With the Higgs boson being responsible for mass generation its couplings to massive SM particles are proportional to their masses:  $g_{FH} = m_f/v$ ,  $g_{VVH} = 2M_V^2/v$ . Thus Higgs bosons decay preferentially into the heaviest kinematically possible final states. State-of-the-art branching ratio calculations including electro-weak and QCD corrections [8] are coded in the program HDECAY [9] for the SM and its minimal supersymmetric extension, the MSSM. Branching ratios of the neutral Higgs bosons in the MSSM can be also calculated with program FeynHiggsDecay [10]. The SM Higgs branching ratios in the mass range relevant to a LC are shown in Fig. 2.

### Tools for Simulation

A variety of leading-order Monte Carlo generators exist which are commonly used for Higgs studies in  $e^+e^-$  collisions. They are PYTHIA [11], HERWIG [12], HZHA [13], CompHep [14], and WHiZard [15]. CompHep and WHiZard offer the possibility of generating the complete  $2 \rightarrow 4$  and (in the case of WHiZard) also  $2 \rightarrow 6$  processes including their interference with SM backgrounds.

\* Most of the work reported in this talk was done by members of the Higgs working group of the Extended ECFA/DESY Study: V. Barger<sup>a</sup>, M. Battaglia<sup>b</sup>, M. Beccaria<sup>c</sup>, E. Boos<sup>d</sup>, J.C. Brent<sup>e</sup>, S.Y. Choi<sup>f</sup>, D. Choudhury<sup>b</sup>, A. Datta<sup>g</sup>, S. Dawson<sup>h</sup>, S. DeCurtis<sup>i</sup>, G. Degrassi<sup>j,k</sup>, A. Denner<sup>l</sup>, A. DeRoeck<sup>b</sup>, N.G. Deshpande<sup>m</sup>, S. Dittmaier<sup>n</sup>, A. Djouadi<sup>o</sup>, D. Dominici<sup>i,p</sup>, M. Dubinin<sup>d</sup>, H. Eberl<sup>q</sup>, J. Ellis<sup>b</sup>, A. Ferrari<sup>r</sup>, M. Frank<sup>s</sup>, E. Gabrielli<sup>g</sup>, A. Gay<sup>t</sup>, I.F. Ginzburg<sup>u</sup>, D.K. Ghosh<sup>m</sup>, E. Gross<sup>v</sup>, J. Guasch<sup>l</sup>, J.F. Gunion<sup>w</sup>, T. Hahn<sup>n</sup>, T. Han<sup>a</sup>, S. Heinemeyer<sup>x</sup>, W. Hollik<sup>n</sup>, K. Huitu<sup>g</sup>, A. Imhof<sup>y,z</sup>, J. Jiang<sup>aa</sup>, A. Kiiiskinen<sup>g</sup>, T. Klimkovich<sup>y,z</sup>, B.A. Kniehl<sup>z</sup>, M. Krawczyk<sup>bb</sup>, T. Kuhl<sup>y</sup>, P. Langacker<sup>cc</sup>, F. Madrigal<sup>y,z</sup>, W. Majerotto<sup>q</sup>, T. Maki<sup>g</sup>, B. McElrath<sup>a</sup>, B. Mele<sup>j,k</sup>, N. Meyer<sup>y,z</sup>, D.J. Miller<sup>b</sup>, S. Moretti<sup>b</sup>, M. Mühlleitner<sup>l</sup>, K. Olive<sup>dd</sup>, P. Osland<sup>ec</sup>, S. Peñaranda<sup>n</sup>, A. Pilaftsis<sup>ff</sup>, A. Raspereza<sup>y</sup>, F.M. Renard<sup>o</sup>, M. Ronan<sup>gg</sup>, M. Roth<sup>n</sup>, H.J. Schreiber<sup>y</sup>, M. Schumacher<sup>hh</sup>, P. Slavich<sup>n,s</sup>, A. Sopczak<sup>ii</sup>, V.C. Spanos<sup>dd</sup>, M. Steinhauser<sup>y</sup>, S. Trimarchi<sup>jj</sup>, C. Verzegnassi<sup>jj</sup>, A. Vologdin<sup>d</sup>, Z. Was<sup>kk</sup>, M.M. Weber<sup>t</sup>, G. Weiglein<sup>ll</sup>, M. Worek<sup>mm</sup>, M. Yao<sup>gg</sup>, P.M. Zerwas<sup>y</sup>, <sup>a</sup> University of Wisconsin, <sup>b</sup> CERN, <sup>c</sup> INFN, University di Lecce, <sup>d</sup> Moscow State University, <sup>e</sup> LPNHE Ecole Polytechnique, <sup>f</sup> Chonbuk National University, <sup>g</sup> Helsinki Institute of Physics, <sup>h</sup> BNL Brookhaven National Laboratory, <sup>i</sup> INFN, Firenze, <sup>j</sup> INFN, Roma, <sup>k</sup> University La Sapienza, Roma, <sup>l</sup> PSI Villigen, <sup>m</sup> University of Oregon, <sup>n</sup> MPI München, <sup>o</sup> Université Montpellier, <sup>p</sup> University of Florence, <sup>q</sup> Inst.f.Hochenergiephysik Oesterr.Akademie d.Wissenschaften, Wien, <sup>r</sup> Uppsala University, <sup>s</sup> University Karlsruhe, <sup>t</sup> IRES Strasbourg, <sup>u</sup> NSC Novosibirsk, <sup>v</sup> Weizmann Institute, <sup>w</sup> University of California, Davis, <sup>x</sup> LMU München, <sup>y</sup> DESY Hamburg, <sup>z</sup> University of Hamburg, <sup>aa</sup> ANL Argonne, <sup>bb</sup> Warsaw University, <sup>cc</sup> University of Pennsylvania, <sup>dd</sup> University of Minnesota, <sup>ee</sup> University of Bergen, <sup>ff</sup> Manchester University, <sup>gg</sup> LBNL Berkeley, <sup>hh</sup> University of Bonn, <sup>ii</sup> Lancaster University, <sup>jj</sup> INFN, University Trieste, <sup>kk</sup> INP Cracow, <sup>ll</sup> University of Durham, <sup>mm</sup> University of Silesia, Katowice.

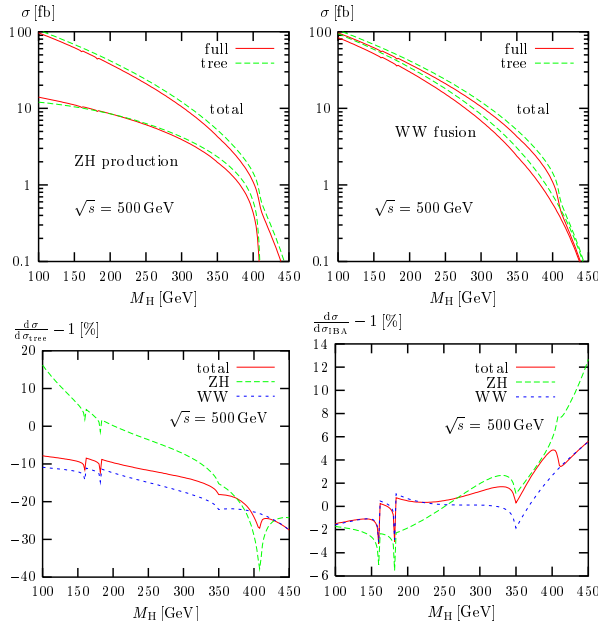


Figure 1: Upper plots: cross-section for the processes  $e^+e^- \rightarrow ZH^0$  and  $e^+e^- \rightarrow \nu_e \bar{\nu}_e H^0$  including complete one-loop electro-weak corrections for  $\sqrt{s} = 500$  GeV. Lower plots: Relative amount of one-loop corrections relative to Born level result (left) and relative to an improved Born approximation (IBA) (from [7]).

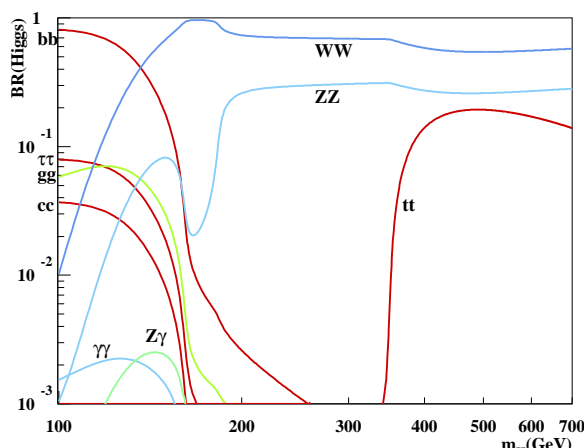


Figure 2: Branching ratios of the SM Higgs boson calculated with HDECAY [9].

Beamstrahlung was simulated in most analyses presented below using the parameterization CIRCE [16].

The vast majority of experimental analyses in this summary includes the simulation of complete SM backgrounds. The effects of limited detector acceptance and resolution have been incorporated using the parametric detector simulation program SIMDET [17] which is based on the de-

tector performance specified for the TESLA detector in the TDR. A comparative study of different event generators and of different fast detector simulation programs was carried out in [18].

Most analyses which involve tagging of heavy quarks use a realistic event-wise neural-net algorithm based on ZVTOP [19] which was first used at the SLD detector.

A detailed simulation (BRAHMS [20]) of the TESLA TDR detector based on GEANT3 along with a reconstruction program is available and can be used for comparative studies.

### Coupling to Z Bosons

The anchor of a model-independent precision analysis of Higgs boson properties at a LC is the measurement of the total cross-section for the Higgs-strahlung process,  $e^+e^- \rightarrow H^0Z$ .  $Z$  bosons can be selected in  $Z \rightarrow e^+e^-$  and  $Z \rightarrow \mu^+\mu^-$  decays. From energy-momentum conservation the invariant mass recoiling against the  $Z$  candidate can be calculated. Through a cut on the recoil mass, Higgs bosons can be selected independent of their decay mode, allowing for a model-independent measurement of the effective  $HZ$  coupling,  $g_{HZZ}$ . Once  $g_{HZZ}$  is known, all other Higgs couplings can be determined absolutely. The total Higgs-strahlung cross-section can be measured with an accuracy of 2.5% for  $m_H = 120$  GeV and  $\sqrt{s} = 350$  GeV for  $500 \text{ fb}^{-1}$  [21]. Assuming that the uncertainty scales with the square root of the cross-section and that the selection purity and efficiency is independent of the center-of-mass energy, one can obtain an accuracy between 1.2 % and 10% for  $100 < m_H < 360$  GeV, for an integrated luminosity of  $\sqrt{s} \times \text{fb}^{-1} / \text{GeV}$  at a center-of-mass energy corresponding to the maximum of the cross-section for a given Higgs mass. The relative error is shown in Fig. 3 together with the optimal center-of-mass energy as a function of the Higgs mass.

The importance of a precise and model-independent determination of  $g_{HZZ}$  has e.g. recently been discussed in the context of supersymmetric models [22] and in the context of models with higher Higgs field representations, as well as in the context of extra-dimensional models [23].

### Quantum Numbers

The measurements of differential production cross-sections and decay angular distributions provide access to the discrete quantum numbers of the Higgs boson:  $J^{PC}$ . In the TDR, the measurement of the  $\beta$ -dependence of the Higgs-strahlung cross-section close to the production threshold was exploited to determine the spin of the Higgs boson. The spin can also be determined from the invariant mass of the off-shell  $Z$  boson in the decay  $H^0 \rightarrow ZZ^*$  for  $m_H < 2m_Z$ . This method is independent of the Higgs production process and thus potentially applicable also in  $\gamma\gamma$  and  $gg$  collisions. The invariant mass distribution for  $m_H = 150$  GeV is shown in Fig. 4. For  $m_H$  above  $2m_Z$ , azimuthal correlations of the two  $Z$  boson decay planes can

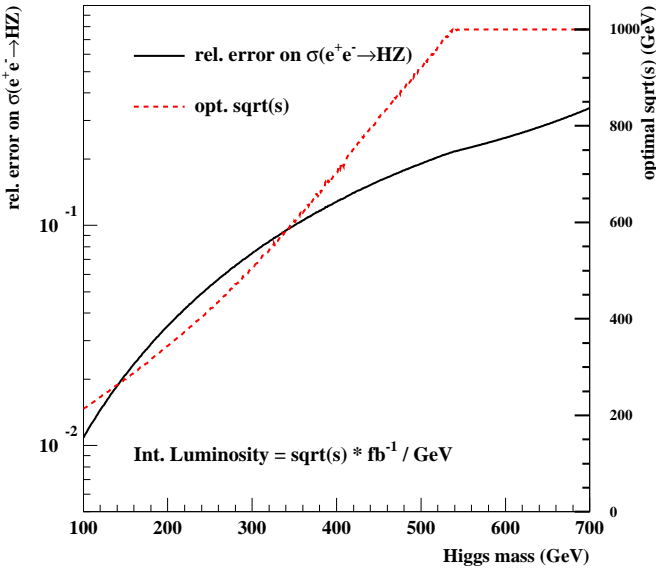


Figure 3: Achievable precision on the cross-section for  $e^+e^- \rightarrow H^0Z$  as a function of the Higgs mass. An integrated luminosity proportional to the center-of-mass energy in  $\text{fb}^{-1}/\text{GeV}$  at a center-of-mass energy corresponding to the maximum of the cross-section is assumed. The center-of-mass energy which yields the largest cross-section is also shown (dashed line, right scale).

be exploited to gain sensitivity to Higgs boson spin and CP [24, 25].

The CP quantum number, like the spin, can be determined from both Higgs boson production and decay [26]. In the TDR, the sensitivity of the angular distribution of the Z recoiling against the  $H^0$  in Higgs-strahlung was exploited. Recently a method has been proposed which makes use of the transverse spin correlation in  $H^0 \rightarrow \tau^+\tau^-$  decays. The spin correlations between the two  $\tau$  leptons is probed through angular correlations of their decay products. In particular, events from  $\tau^\pm \rightarrow \rho^\pm \nu_\tau \rightarrow \pi^\pm \pi^0 \nu_\tau$  and from  $\tau^\pm \rightarrow a_1^\pm \nu_\tau \rightarrow \rho^0 \pi^\pm \nu_\tau \rightarrow \pi^\pm \pi^\mp \pi^\pm \nu_\tau$  can be used. The angle between the decay planes of the two  $\rho$  mesons from either  $\tau$  decay provides a suitable observable [27, 28]. While this angle can be determined in the laboratory frame, ideally it is evaluated in the Higgs boson rest frame, which can be approximately reconstructed using  $\tau$  lifetime information [29]. Preliminary results including detector simulation have shown that from a sample of  $1 \text{ ab}^{-1}$  of Higgs-strahlung events at  $\sqrt{s} = 350 \text{ GeV}$ , a statistical separation between a CP-even and a CP-odd Higgs boson of eight standard deviations may be achieved assuming production cross section and branching ratio as for  $H^0_{\text{SM}}$  (see Fig. 5, note that background is not yet taken into account) [30].

### Decay Branching Ratios

The precise measurement of Higgs boson decay branching ratios is one of the key tasks in LC Higgs physics. In

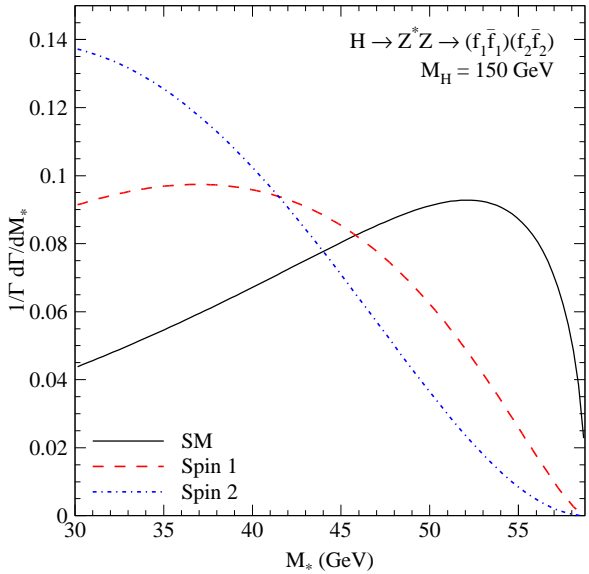


Figure 4: Distribution of the invariant mass of the decay products of the off-shell  $Z^*$  boson in  $H^0 \rightarrow ZZ^*$  decays for the SM Higgs and for examples of spin-1 and spin-2 bosons for  $m_H = 150 \text{ GeV}$  (from [25]).

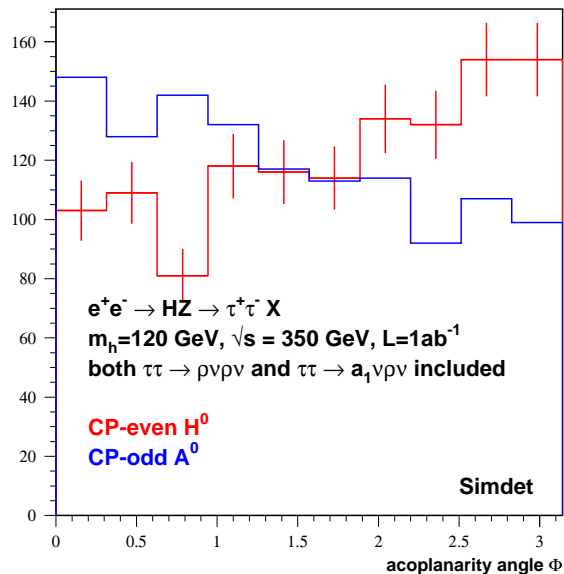


Figure 5: Acoplanarity angle between the two  $\rho$  decay planes from  $H^0/A^0 \rightarrow \tau^+\tau^-$  decays (from [30]).

the TESLA TDR as well as in all other regional LC studies [31, 32] analyses have been performed to investigate the expected precisions on the branching ratio determination. For a light Higgs boson with  $m_H < 160 \text{ GeV}$ , a large variety of Higgs decay modes can be measured. The hadronic decays into  $b\bar{b}$ ,  $c\bar{c}$ , and  $gg$  are disentangled via the excellent capabilities of a LC vertex detector. Progress has been achieved recently in the level of detail at which the algorithms to tag  $b$ - and  $c$ -quarks are implemented into the simulation. Although these studies are not finished, it

looks conceivable that the results of the TDR study will essentially be confirmed [33].

There are two different methods to extract branching ratios from the observed events:

1. Measure the topological cross-section for a given final state, e.g.  $\sigma(H^0 Z \rightarrow X Z)$  and divide by the total measured Higgs–strahlung cross-section (as obtained from the recoil mass measurement) [34].
2. Select a sample of unbiased  $H^0 Z$  events (events in the recoil mass peak) and determine the fraction of events corresponding to a given  $H^0 \rightarrow X$  decay within this sample.

The latter method was first applied to Higgs branching ratio studies in [35]. Since in this approach binomial (or in principle multi-nomial) statistics can be applied, smaller errors of the branching ratios can be inferred for the same number of events than from a rate measurement. Although only relying on events with  $Z \rightarrow \ell^+ \ell^-$ , the latter method yields errors very similar to those of the TDR method [34]. The achievable precision for the both methods for a SM Higgs boson of 120 GeV from a sample of  $500 \text{ fb}^{-1}$  is shown in Table 1. A possible combination of both methods is currently being investigated. While for the hadronic Higgs decays, there is a sizable overlap, for the  $H^0 \rightarrow W^+ W^-$  decay a significant improvement may be expected from combination.

Besides the decays into  $b\bar{b}$ ,  $c\bar{c}$ ,  $gg$ ,  $\tau^+ \tau^-$ ,  $W^+ W^-$ ,  $Z^0 Z^0$ , and  $\gamma\gamma$  further decay modes have been studied. The very rare decay  $H^0 \rightarrow \mu^+ \mu^-$  might be detectable in WW-fusion events at  $\sqrt{s} = 800$  GeV for  $m_H = 120$  GeV. A measurement of the muon Yukawa coupling with approximately 15% relative accuracy may be obtained from a sample of  $1 \text{ ab}^{-1}$ . Here, the logarithmic rise of the signal cross-section with  $\sqrt{s}$  is of advantage. A precision measurement of the  $H^0 \rightarrow \mu^+ \mu^-$  branching ratio however can only be performed at even higher luminosity or at higher energy [36]. The expected signal is shown in Fig. 6.

Another rare Higgs boson decay is the loop-induced  $H^0 \rightarrow Z\gamma$  decay. This decay has been studied in the  $WW \rightarrow H^0 \rightarrow q\bar{q}\gamma$  final state for a sample of  $1 \text{ ab}^{-1}$  at 500 GeV for  $120 \text{ GeV} < m_H < 160 \text{ GeV}$ . Around the expected maximum of the branching ratio for a SM Higgs boson (140 GeV), a relative error of 27% can be expected while for lower (120 GeV) and higher (160 GeV) Higgs masses only upper limits at 70-80% of the SM branching ratio can be expected to be set [37]. The expected signal is shown in Fig. 7 together with the background.

### Invisible Higgs Decays

In the TDR it was pointed out that the decay independent recoil mass technique allows us to extract a possible invisible decay width of the Higgs boson by comparing the rate of events in the recoil mass peak with the rate for all visible decays. This indirect technique is now complemented by a study which explicitly asks for missing energy and

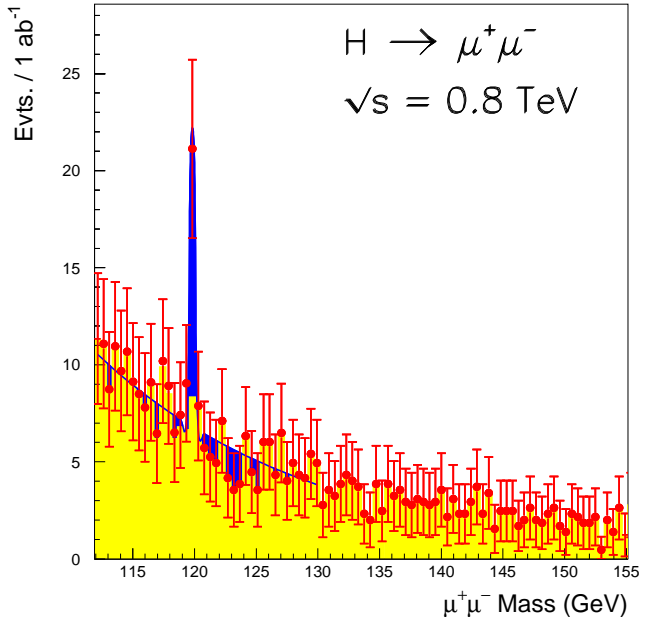


Figure 6: Expected mass spectrum for the decay  $H^0 \rightarrow \mu^+ \mu^-$  from a sample of  $1 \text{ ab}^{-1}$  at  $\sqrt{s} = 800$  GeV for  $m_H = 120$  GeV (from [36]).

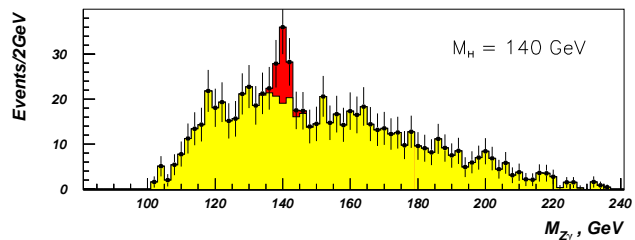


Figure 7: Expected mass spectrum for the decay  $H^0 \rightarrow Z\gamma$  from a sample of  $1 \text{ ab}^{-1}$  at  $\sqrt{s} = 500$  GeV for  $m_H = 120$  GeV (from [37]).

momentum compatible with an invisible Higgs decay. At  $\sqrt{s} = 350$  GeV, the achievable precision on the invisible branching ratio is shown to be significantly higher than in the indirect approach, yielding e.g. a relative precision of  $\sim 10\%$  for a branching ratio of 5% and a  $5\sigma$  observation down to a branching ratio of 1.5-2.0% with  $500 \text{ fb}^{-1}$  at  $\sqrt{s} = 350$  GeV and Higgs masses between 120 and 160 GeV [38] (see Fig. 8).

### Heavier SM Higgs Boson

Above a Higgs mass of approximately  $2 m_W$ , the phenomenology of the SM Higgs changes quite drastically. First, the bosonic decays into  $W^+ W^-$  and  $ZZ$  rapidly become dominant, leaving only very little room for Yukawa couplings to be probed directly. Second, the total decay width increases rapidly with mass, exceeding 1 GeV for  $m_H > 190$  GeV.

In order to assess the question up to which Higgs mass a

Table 1: Summary of expected precisions on Higgs boson branching ratios from existing studies within the ECFA/DESY workshops. (a) for  $500 \text{ fb}^{-1}$  at 350 GeV; (b) for  $500 \text{ fb}^{-1}$  at 500 GeV; (c) for  $1 \text{ ab}^{-1}$  at 500 GeV; (d) for  $1 \text{ ab}^{-1}$  at 800 GeV; (e) as for (a), but method described in [35] (see text).

Mass(GeV)	120	140	160	180	200	220	240	280	320
Decay	Relative Precision (%)								
bb	2.4 (a) / 1.9 (e)	2.6 (a)	6.5 (a)	12.0 (d)	17.0 (d)	28.0 (d)			
c <bar>c</bar>	8.3 (a) / 8.1 (e)	19.0 (a)							
$\tau\tau$	5.0 (a) / 7.1 (e)	8.0 (a)							
$\mu\mu$	30. (d)								
gg	5.5 (a) / 4.8 (e)	14.0 (a)							
WW	5.1 (a) / 3.6 (e)	2.5 (a)	2.1 (a)						
ZZ			16.9 (a)						
$\gamma\gamma$	23.0 (a) / 35.0 (e)		27.0 (c)						
Z $\gamma$					3.5 (b)			5.0 (b)	7.7 (b)
					9.9 (b)			10.8 (b)	17.3 (b)

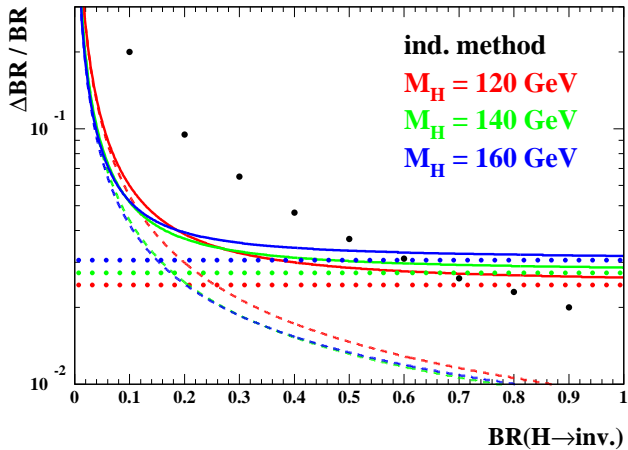


Figure 8: Accuracy on the branching ratio  $H^0 \rightarrow \text{invisible}$ , as a function of  $BR(H^0 \rightarrow \text{invisible})$  for three Higgs masses using  $500 \text{ fb}^{-1}$  at 350 GeV (full line). The dashed and dotted lines indicate the contributions from the measurement of the invisible rate and from the total Higgs-strahlung cross section measurement, respectively. The large dots are the result of the indirect method, presented in the TDR (from [38]).

direct Yukawa coupling measurement would still be possible, a study was performed which aims at selecting  $H^0 \rightarrow b\bar{b}$  as a rare Higgs decay [39]. Like in the case of  $H^0 \rightarrow \mu^+\mu^-$ , the large number of Higgs bosons produced in the WW-fusion channel at high energy is favorable in comparison to using the Higgs-strahlung process at lower energies. For  $1\text{ab}^{-1}$  of data at  $\sqrt{s} = 800 \text{ GeV}$ , a  $5\sigma$  sensitivity to the bottom Yukawa coupling is achievable for  $m_H < 210 \text{ GeV}$ . A measurement of the branching ratio  $BR(H^0 \rightarrow b\bar{b})$  is possible with (12,17,28) % accuracy for  $m_H = (180,200,220) \text{ GeV}$ .

The second question about heavier Higgs bosons is, whether the Higgs line-shape parameters (mass, decay

width, Higgs-strahlung production cross section) can be measured. A complete study of the mass range  $200 \text{ GeV} < m_H < 320 \text{ GeV}$  has been performed [40]. The final state  $q\bar{q}q\bar{q}\ell^+\ell^-$  resulting from  $H^0Z \rightarrow ZZZ$  and from  $H^0Z \rightarrow W^+W^-Z$  is selected. A kinematic fit is used to assign the possible di-jet combinations to bosons ( $W^+W^-$  or  $ZZ$ ). The resulting di-boson mass spectrum can be fitted by a Breit-Wigner distribution convoluted with a detector resolution function. A relative uncertainty on the Higgs mass of 0.11 – 0.36 % is achievable from  $500 \text{ fb}^{-1}$  at 500 GeV for masses between 200 and 320 GeV. The resolution on the total width varies between 22 and 34% for the same mass range. Finally, the total Higgs-strahlung cross-section can be measured with 3.5 – 6.3% precision. Under the assumption that only  $H^0 \rightarrow W^+W^-$  and  $H^0 \rightarrow ZZ$  decays are relevant, their branching ratios can be extracted with 3.5–8.6% and 9.9–17.3%, respectively (see Table 2). The expected mass spectra for  $m_H = 200 \text{ GeV}$  and  $m_H = 320 \text{ GeV}$  are shown in Fig. 9.

Table 2: Expected precision on Higgs boson line-shape parameters for  $200 < m_H < 320 \text{ GeV}$  at a LC with  $\sqrt{s} = 500 \text{ GeV}$ .

$m_H$ (GeV)	$\Delta\sigma$ (%)	$\Delta m_H$ (%)	$\Delta\Gamma_H$ (%)
200	3.6	0.11	34
240	3.8	0.17	27
280	4.4	0.24	23
320	6.3	0.36	26

### Top Yukawa Coupling

For  $m_H < 2m_t$ , the top quark Yukawa coupling is not directly accessible from Higgs decays. The only relevant tree level process to access the top quark Yukawa coupling is the process  $e^+e^- \rightarrow H^0t\bar{t}$  [41]. Due to the large

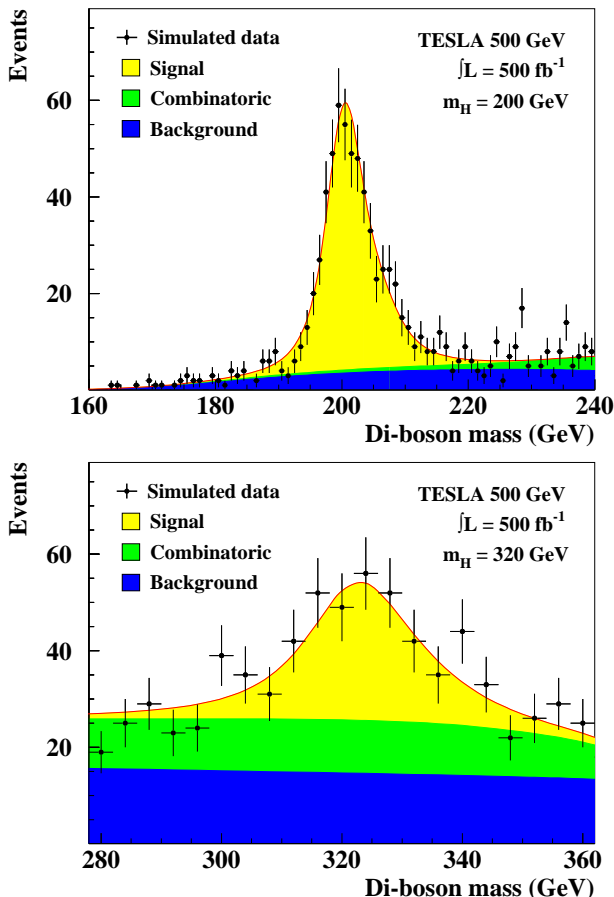


Figure 9: Expected reconstructed Higgs boson mass spectra for  $m_H = 200$  GeV and  $m_H = 320$  GeV from  $500 \text{ fb}^{-1}$  at 500 GeV (from [40]).

masses of the final state particles, the process only has a significant cross-section at center-of-mass energies significantly beyond 500 GeV. Higher order QCD corrections to the process have been calculated and are significant [42]. Recently, also the full  $\mathcal{O}(\alpha)$  electro-weak corrections became available [43]. Experimental studies have been performed for  $m_H < 130$  GeV in the TDR [44] and in the NLC study [45]. Recently a completely new study has been performed with refined b-tagging simulation as well as for an extended mass range of up to  $m_H = 200$  GeV, exploiting also the  $H^0 \rightarrow W^+W^-$  decay [46]. For the  $H^0 \rightarrow bb$  case, both the  $t\bar{t} \rightarrow bbq\bar{q}\ell^-\bar{\nu}$  and the  $t\bar{t} \rightarrow bb\bar{q}q\bar{q}$  channels have been analyzed. For the  $H^0 \rightarrow W^+W^-$  case, the 2-like-sign lepton plus 6-jet and the single lepton plus 8-jet final states were studied. The events were selected by neural networks. The generic 6-fermion background is fully taken into account. The expected uncertainties on the top Yukawa coupling for  $1\text{ab}^{-1}$  at 800 GeV range from 6–14% for  $120 < m_H < 200$  GeV and are shown in Fig. 10.

### Higgs Potential

The observation of a non-zero self-coupling of the Higgs boson is the ultimate proof of spontaneous symmetry breaking being responsible for mass generation of the SM bosons and fermions since it probes the shape of the Higgs potential and thus the presence of a vacuum expectation value. Higgs boson self-coupling in general leads to triple and quartic Higgs boson couplings out of which only the former is accessible. For 500 GeV center-of-mass energy, the double Higgs-strahlung process,  $e^+e^- \rightarrow H^0H^0Z$  is most promising for observation, the small cross-section of 0.1 – 0.2 fb however demands the highest possible luminosity and calls for ultimate jet energy resolution since only if the most frequent six jet final state  $bb\bar{b}\bar{b}q\bar{q}$  can be reconstructed, the signal rate becomes significant. The cross-section has been calculated in [47]. In the TDR, an experimental analysis for  $m_H = 120$  GeV was presented [48] which concluded that with  $1\text{ab}^{-1}$  of data at 500 GeV, a precision of 17 – 23 % for  $120 < m_H < 140$  GeV on the  $e^+e^- \rightarrow H^0H^0Z$  cross-section can be achieved. Recently, the potential of the WW-fusion channel for higher Higgs boson masses at higher energies was discussed and compared to the possibilities at the LHC in [49]. Furthermore, it was discussed how the existing analyses might be improved by exploiting kinematic differences between the signal diagram and diagrams which lead to the same final state without involving the triple Higgs coupling (dilution diagrams), namely the sequential radiation of two Higgs bosons from one Z boson and the diagram which involves the quartic ZZHH coupling [50]. In particular, the invariant mass of the hadronic system which is formed by the two Higgs boson decay products is sensitive to the different contributions to the HHZ final state. Its distribution is shown in Fig. 11. A reduction of the uncertainty on the trilinear coupling from 0.23 to 0.20 can be obtained.

## MINIMAL SUPERSYMMETRIC HIGGS SECTOR

### Theoretical Predictions

The Higgs sector of the Minimal Supersymmetric Standard Model (MSSM) comprises two complex scalar field doublets which acquire vacuum expectation values  $v_1$  and  $v_2$ . After electro-weak symmetry breaking, two charged Higgs bosons ( $H^\pm$ ) and three neutral Higgs bosons emerge, two of which are CP-even ( $h^0, H^0$ ) and one is CP-odd ( $A^0$ ), if CP is conserved. In contrast to the SM, the Higgs masses are predicted in terms of the fundamental parameters of the MSSM. At tree level, the mass spectrum is determined by  $\tan\beta = v_2/v_1$  and  $m_A$  and the mass of the  $h^0$  has to fulfill  $m_h < m_Z$ . Higher order corrections, predominantly from loops involving third generation fermions and their supersymmetric partners, have large influence. In particular,  $m_h$  can be as large as 135 GeV [51]. A compilation of more recent higher order corrections can be found in [52]. The value of  $m_h$  as a function of  $\tan\beta$  is shown for two

- $H \rightarrow bb$  semilep;  $\Delta\sigma_{BG}^{eff}/\sigma_{BG}^{eff} = 5\%$
- $H \rightarrow bb$  semilep;  $\Delta\sigma_{BG}^{eff}/\sigma_{BG}^{eff} = 10\%$
- $H \rightarrow bb$  hadro;  $\Delta\sigma_{BG}^{eff}/\sigma_{BG}^{eff} = 5\%$
- $H \rightarrow bb$  hadro;  $\Delta\sigma_{BG}^{eff}/\sigma_{BG}^{eff} = 10\%$
- $H \rightarrow WW$  2 like sign lep;  $\Delta\sigma_{BG}^{eff}/\sigma_{BG}^{eff} = 5\%$
- $H \rightarrow WW$  2 like sign lep;  $\Delta\sigma_{BG}^{eff}/\sigma_{BG}^{eff} = 10\%$
- $H \rightarrow WW$  1 lep;  $\Delta\sigma_{BG}^{eff}/\sigma_{BG}^{eff} = 5\%$
- $H \rightarrow WW$  1 lep;  $\Delta\sigma_{BG}^{eff}/\sigma_{BG}^{eff} = 10\%$
- $4$  channels combined;  $\Delta\sigma_{BG}^{eff}/\sigma_{BG}^{eff} = 5\%$
- $4$  channels combined;  $\Delta\sigma_{BG}^{eff}/\sigma_{BG}^{eff} = 10\%$

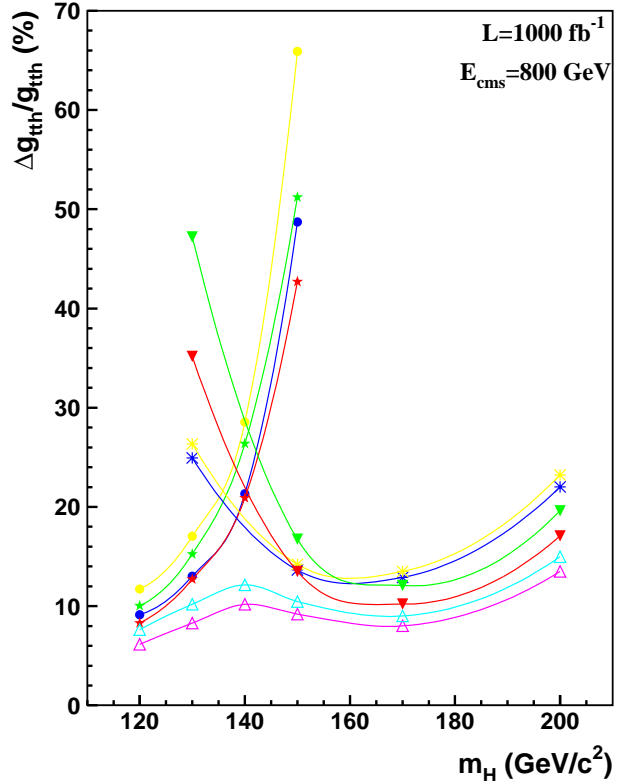


Figure 10: Expected relative precision on the top Yukawa coupling for  $120 < m_H < 200$  GeV from  $1 \text{ ab}^{-1}$  at 800 GeV for various final states and for two different assumptions of the systematic uncertainty on the background (BG) normalization (from [46]).

different cases of scalar-top mixing (no-mixing and  $m_h^{\max}$  scenarios of [55]) in Fig. 12. The complete 1-loop and dominant 2-loop SUSY corrections to the production cross-sections for  $e^+e^- \rightarrow h^0Z$  [53, 54] and the 1-loop corrections from stop-sbottom loops for  $e^+e^- \rightarrow \nu_e\bar{\nu}_e h^0$  [56, 57] are calculated.

The MSSM Higgs sector exhibits a so-called decoupling limit as  $m_A$  becomes large, in which the  $h^0$  approaches the properties of the SM Higgs boson [58]. This limit is approached relatively fast for  $m_A > 200$  GeV in a large portion of the MSSM parameter space. However, also scenarios far away from decoupling (e.g. *the intense coupling scenario* [59]) is experimentally not excluded and theoretically possible. In such a scenario, all Higgs bosons are accessible already at 500 GeV and a rich phenomenology is waiting to be disentangled. The closer the MSSM scenario moves towards the decoupling limit the more difficult it becomes to distinguish the Higgs sector from the SM. Therefore most analyses focus on a close-to-decoupling scenario. In this case, the analyses for a light SM Higgs apply also for  $h^0$ . It is the task of the LC to employ the precise measurements of the properties of this lightest Higgs boson to distinguish it from a SM Higgs and draw conclusions on the supersymmetric parameters.

### Study of Heavy Neutral SUSY Higgs Bosons

If  $\cos^2(\beta - \alpha)$  is small<sup>1</sup>, the heavy neutral MSSM Higgs bosons are predominantly produced through the process,  $e^+e^- \rightarrow H^0A^0$ . With the mass splitting between  $H^0$  and  $A^0$  being small for a large part of the parameter space, the mass reach of the LC for  $H^0$  and  $A^0$  is approximately  $\sqrt{s}/2$ . In this case, the coupling of the  $H^0$  to gauge bosons is small, therefore the dominant decays of both  $H^0$  and  $A^0$  are  $b\bar{b}$  and  $\tau^+\tau^-$ . During the workshop, a new experimental study was started to fully determine the sensitivity of the LC to the heavy MSSM Higgs bosons through the pair production process [61]. For the first time, both the  $bbbb$  and  $b\bar{b}\tau^+\tau^-$  final states are analyzed including detector simulation and complete standard model backgrounds. Preliminary results at 500 GeV and 800 GeV center-of-mass energy were obtained. The following assumptions are made:  $500 \text{ fb}^{-1}$  at 500 GeV and at 800 GeV,  $\cos^2(\beta - \alpha) = 0$ ,  $\text{BR}(H^0 \rightarrow b\bar{b}) = 90\%$ ,  $\text{BR}(H^0 \rightarrow \tau^+\tau^-) = 10\%$ . Mass reconstruction is performed using a kinematic fit which imposes energy-momentum conservation. Therefore a good mass reconstruction is achieved both in the  $bbbb$  and  $b\bar{b}\tau^+\tau^-$  final states, see Fig. 13 and 14. The achievable precisions on masses and topological cross-sections are listed in Table 3 for various choices of  $m_H$  and  $m_A$ .

<sup>1</sup>  $\alpha$  is the mixing angle in the CP-even neutral Higgs sector

Table 3: Expected precision on the properties of heavy MSSM Higgs bosons from  $500 \text{ fb}^{-1}$  at 500 GeV (a) and 800 GeV (b), respectively (from [61]).

	$m_A$ (GeV)	$m_H$ (GeV)	precision on			
			$(m_A + m_H)$ (GeV)	$( m_A - m_H )$ (GeV)	$\sigma(bbbb)$ (GeV)	$\sigma(bb\tau^+\tau^-)/\sigma(\tau^+\tau^-bb)$ (%)
			(GeV)	(GeV)	(%)	(%)
(a)	140	150	0.2	0.2	1.5	7.2/6.3
(a)	150	200	0.3	0.4	2.3	9.7/8.7
(a)	200	200	0.4	0.4	2.7	8.1
(a)	200	250	0.4	1.2	6.5	-
(b)	250	300	0.5	0.7	3.0	13.8/11.9
(b)	300	300	0.6	0.7	3.5	10.0
(b)	300	400	1.9	2.8	7.0	-

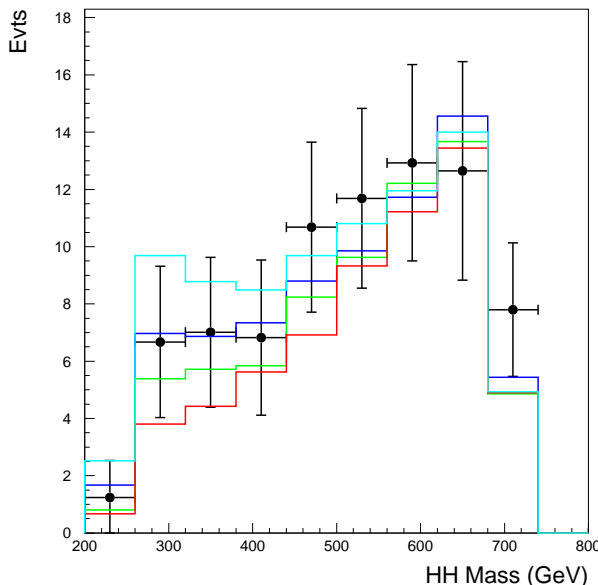


Figure 11: Distribution of the  $H^0H^0$  invariant mass in  $e^+e^- \rightarrow H^0H^0Z$  events for  $m_H = 120 \text{ GeV}$  ( $1 \text{ ab}^{-1}$  at 800 GeV). The histograms are for predictions of the trilinear Higgs coupling ranging from 1.25 to 0.5 (top to bottom) times the SM coupling. (from [50]).

Since at the tree level and in the decoupling limit the heavy neutral MSSM Higgs bosons decouple from the  $Z$ , the mass reach for their discovery at a LC is limited to approximately  $\sqrt{s}/2$  from the pair production process. It has been investigated during the workshop, how single production mechanisms could extend the mass reach of an  $e^+e^-$  LC. In particular, the WW-fusion process  $e^+e^- \rightarrow \nu_e \bar{\nu}_e H^0$  has been investigated [56]. Its tree level cross-section is proportional to  $\cos(\beta - \alpha)$ . Depending on the SUSY parameters, radiative corrections might increase the cross-section for  $e^+e^- \rightarrow \nu_e \bar{\nu}_e H^0$ , possibly allowing discovery beyond the pair production kinematic limit for certain choices of the MSSM parameters. Using left-polarized electron beams and right-polarized positron

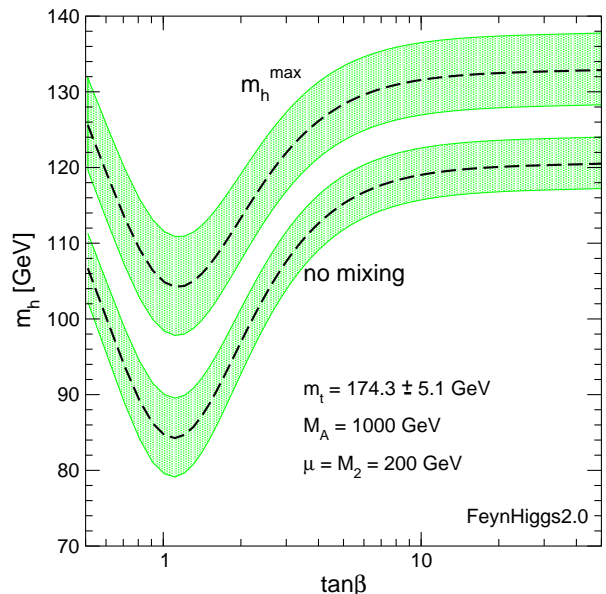


Figure 12: Largest mass of the light CP even Higgs boson of the MSSM as a function of  $\tan\beta$  for two scenarios of scalar-top mixing (no-mixing and  $m_h^{\max}$  scenarios of [55]). The bands indicate the effect of varying the top quark mass by 1 standard deviation of its current error.

beams the cross-section can further be enhanced. A particular scenario where this is the case has been chosen in [56] ( $M_{\text{SUSY}} = 350 \text{ GeV}$ ,  $\mu = 1000 \text{ GeV}$ ,  $M_2 = 200 \text{ GeV}$  and large stop mixing). Cross-section contours for this scenario are shown in Fig. 15.

### Charged Higgs Bosons

Charged Higgs bosons can be pair-produced at the LC via  $e^+e^- \rightarrow H^+H^-$  if  $m_{H^\pm} < \sqrt{s}/2$ . A complete simulation of this process for the decay  $H^+ \rightarrow t\bar{b}$  has been performed for  $\sqrt{s} = 800 \text{ GeV}$ ,  $1 \text{ ab}^{-1}$ , and  $m_{H^\pm} = 300 \text{ GeV}$  [62]. The expected signal and background are shown in Fig. 16. The mass resolution is approximately 1.5%. A  $5\sigma$  discovery will be possible for  $m_{H^\pm} < 350 \text{ GeV}$ .

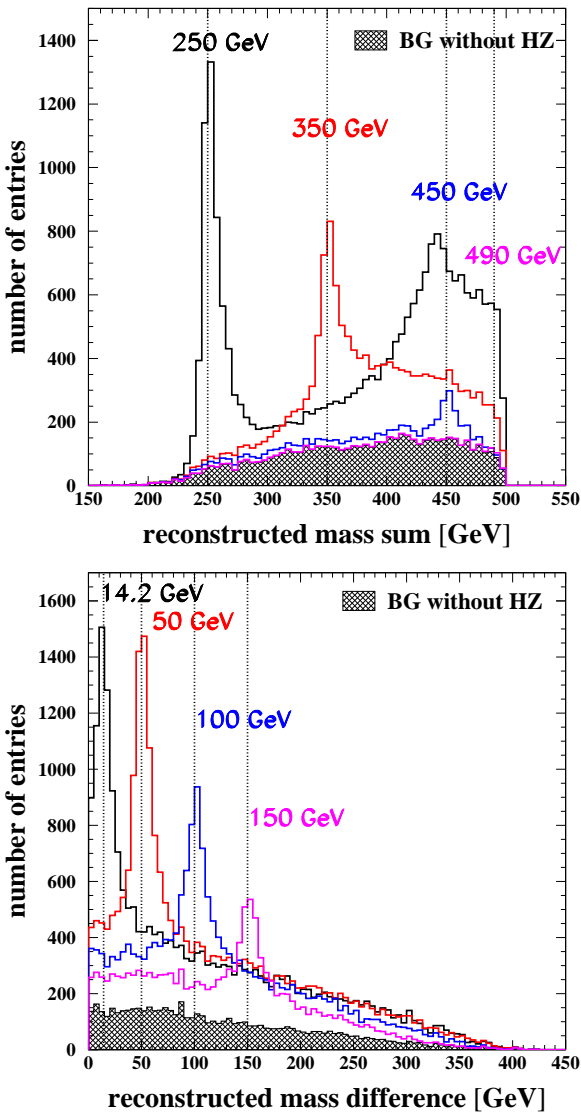


Figure 13: Simulated signals and background of the process  $e^+e^- \rightarrow H^0 A^0 \rightarrow b\bar{b}b\bar{b}$ . Top: reconstructed sum of the two Higgs candidate masses. Bottom: reconstructed difference of the two Higgs boson candidate masses. The study was performed at 500 GeV center-of-mass energy and for  $500\text{fb}^{-1}$ .  $\text{BR}(H^0 \rightarrow b\bar{b}) = \text{BR}(A^0 \rightarrow b\bar{b}) = 0.9$  was assumed (from [61]).

Since in pair production the mass reach for charged Higgs bosons is limited to  $\sqrt{s}/2$ , also the rare processes of single charged Higgs production may be considered. The dominant processes for single charged Higgs production are  $e^+e^- \rightarrow b\bar{t}H^+$ ,  $e^+e^- \rightarrow \tau^-\bar{\nu}_\tau H^+$ , and  $e^+e^- \rightarrow W^-H^+$ . Their cross-sections have been calculated at leading order in [63]. QCD corrections to  $e^+e^- \rightarrow b\bar{t}H^+$  have recently become available [64] and are sizable. In general, parameter regions for which the production cross-section exceeds 0.1 fb are rather small for charged Higgs masses beyond the pair production threshold. Cross-section contours for  $\sqrt{s} = 500$  GeV and 800 GeV are shown in

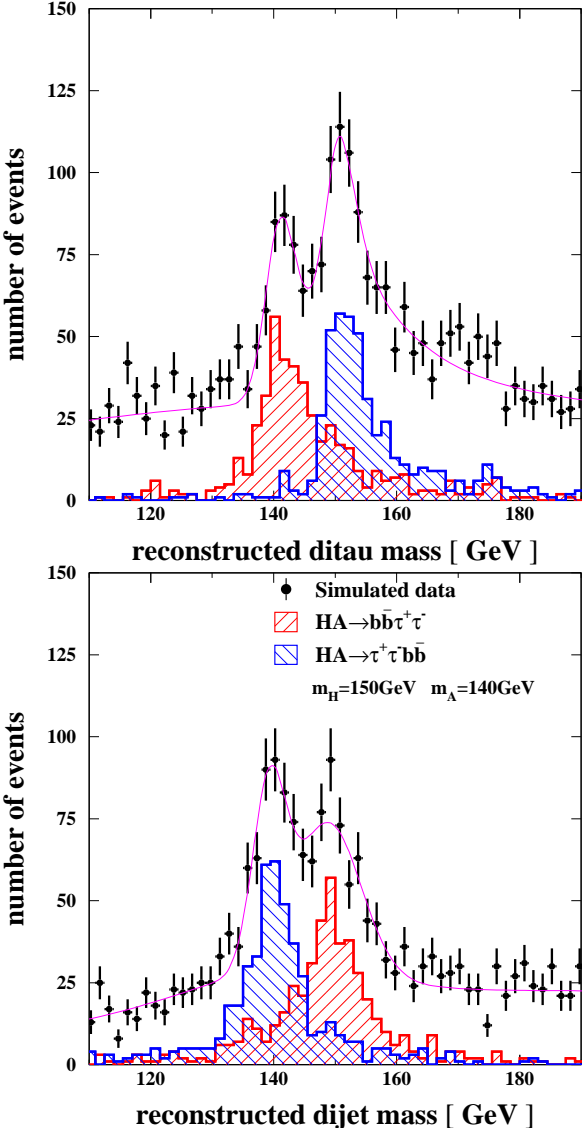


Figure 14: Simulated signal and background of the process  $e^+e^- \rightarrow H^0 A^0 \rightarrow b\bar{b}\tau^+\tau^- (\tau^+\tau^- b\bar{b})$  for  $m_A = 140$  GeV and  $m_H = 150$  GeV at 500 GeV center-of-mass energy ( $500\text{fb}^{-1}$ ). Top: reconstructed  $\tau\tau$  invariant mass from a kinematic fit. Bottom: reconstructed  $b\bar{b}$  invariant mass from a kinematic fit.  $\text{BR}(H^0 \rightarrow \tau^+\tau^-) = \text{BR}(A^0 \rightarrow \tau^+\tau^-) = 0.1$  was assumed (from [61]).

Fig. 17.

### Constraints on SUSY Parameters

At tree level, the MSSM Higgs sector only depends on  $\tan\beta$  and  $m_A$ . Thus, if  $m_A$  would be measured,  $\tan\beta$  could in principle be uniquely determined from the observed Higgs properties. In particular, the coupling of  $A^0$  to down-type fermions is directly proportional to  $\tan\beta$ . Therefore this coupling which appears in the rate of the  $e^+e^- \rightarrow b\bar{b}A^0$  and  $e^+e^- \rightarrow A^0H^0 \rightarrow b\bar{b}b\bar{b}$  processes, as well as in the total decay width  $\Gamma_A$  can be used to extract

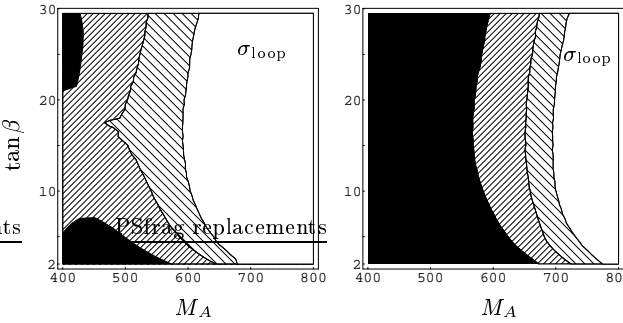


Figure 15: Cross-section contours for  $e^+e^- \rightarrow H^0\nu\bar{\nu}$  for a particular MSSM scenario (see text) in the  $m_A - \tan\beta$ -plane for  $\sqrt{s} = 1$  TeV. The different shadings correspond to: white:  $\sigma \leq 0.01\text{fb}$ , light shaded:  $0.01\text{fb} \leq \sigma \leq 0.02\text{fb}$ , dark shaded:  $0.02\text{fb} \leq \sigma \leq 0.05\text{fb}$ , black:  $\sigma \geq 0.05\text{fb}$  (from [56]). The left figure is for unpolarized beams, the right figure for an electron (positron) polarization of 0.8 (0.6).

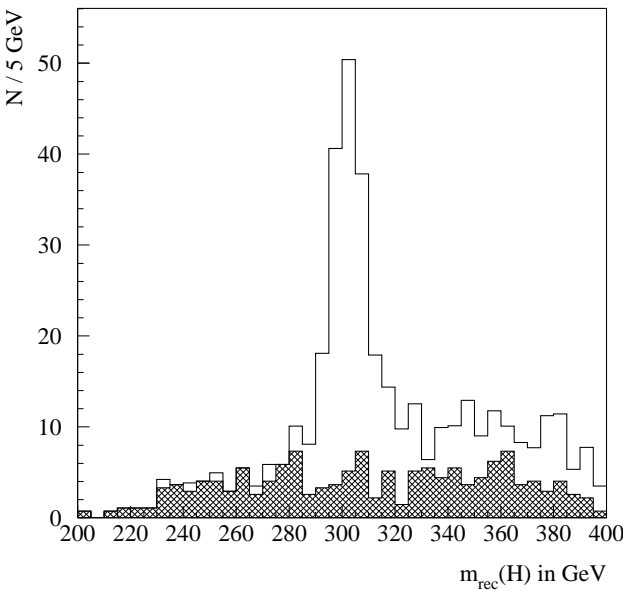


Figure 16: Simulated signal and background of the process  $e^+e^- \rightarrow H^+H^- \rightarrow t\bar{t}t\bar{t}$  for  $m_{H^\pm} = 300$  GeV at 800 GeV center-of-mass energy ( $1\text{ab}^{-1}$ ) (from [62]).

$\tan\beta$  in principle. This has been studied in [66]. Due to the large radiative corrections the predictions for the observables also depend on other SUSY parameters (in particular the sfermion masses and mixings) which are fixed in this analysis. Therefore the resulting errors (see 18) are only valid if all other SUSY parameters, were precisely known.

A different approach to  $\tan\beta$  determination has been proposed in [67]. In a scenario where all SUSY particles are light compared to the center-of-mass energy, the dependence of the cross-section for charged Higgs production on  $\sqrt{s}$  in the 1 TeV domain can be compared to the logarithmic Sudakov expansion of the cross-section. In particular, it has been shown, that the first coefficient of the expansion

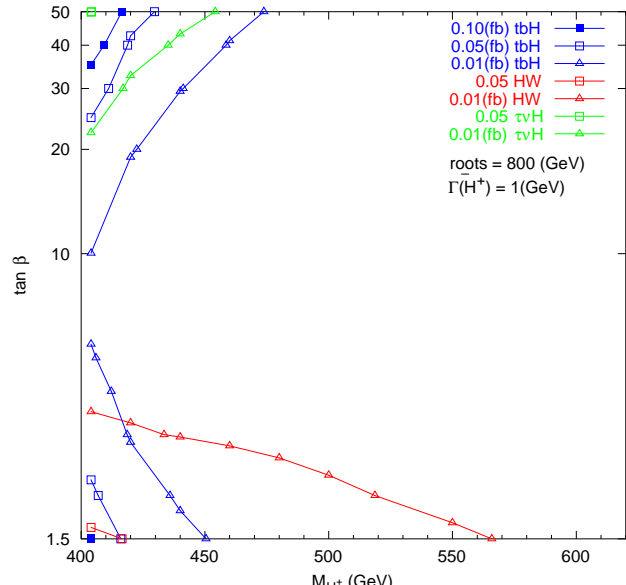
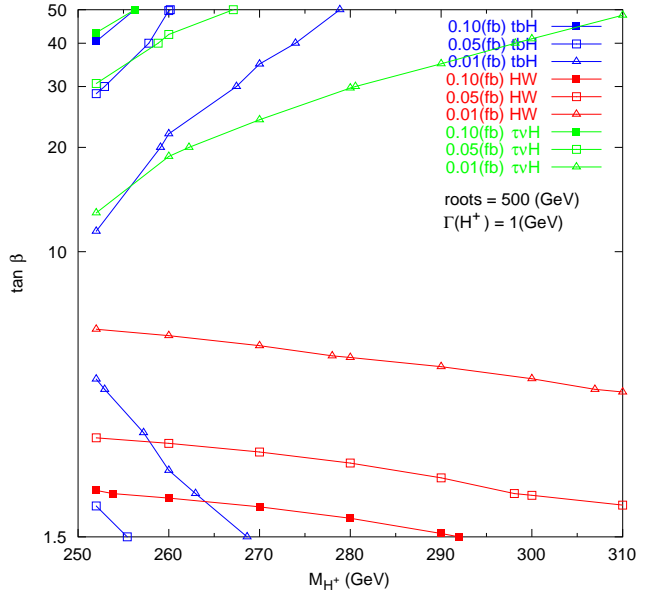


Figure 17: Cross-section contours for the processes  $e^+e^- \rightarrow b\bar{t}H^+$  (blue/dark),  $e^+e^- \rightarrow \tau^-\bar{\nu}_\tau H^+$  (green/light grey), and  $e^+e^- \rightarrow W^-H^+$  (red/medium grey) at  $\sqrt{s} = 500$  GeV (upper) and at 800 GeV (lower). (from [65]).

depends only on  $\tan\beta$ .

A complete study of SUSY parameter determination in the full MSSM is only possible when studies of the Higgs sector are combined with information on sparticle production. Within more constrained SUSY models which assume specific SUSY breaking schemes Higgs observables alone can lead to significant constraints [68]. As an example, the NUHM (non-universal Higgs mass) model has been considered in [69]. The NUHM model assumes unification of sfermion masses and mixing terms as well as unification of gaugino mass terms at a high scale. However, in con-

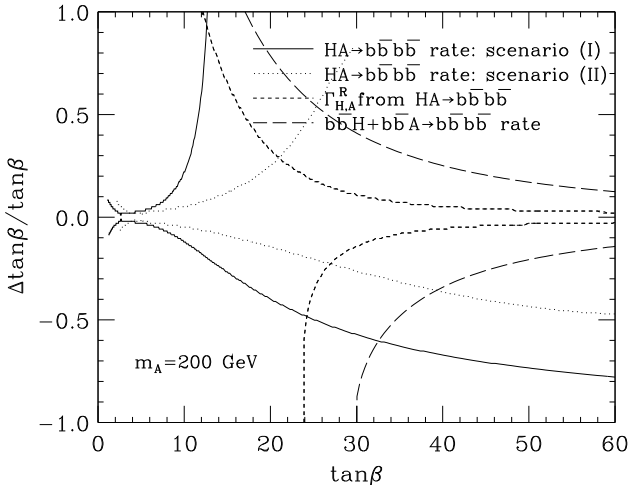


Figure 18: Sensitivity of the  $e^+e^- \rightarrow H^0 A^0 \rightarrow b\bar{b}b\bar{b}$  and  $e^+e^- \rightarrow b\bar{b}A^0/H^0$  cross-sections and the total decay widths  $\Gamma_{H/A}$  on  $\tan\beta$ . Assumed measurement errors are for  $2 \text{ ab}^{-1}$  at 500 GeV without detector simulation (except for  $e^+e^- \rightarrow b\bar{b}A^0/H^0$ ).  $m_A = m_H = m_{H^\pm} = 200 \text{ GeV}$  and all SUSY parameters except  $\tan\beta$  are fixed (from [66]).

trast to the mSUGRA (minimal supergravity) model, both  $\mu$  and  $m_A$  are free parameters. In Fig. 19, the deviation of branching ratios of the lightest Higgs boson from the SM is shown for the NUHM scenario as a function of  $m_A$ . The deviation is plotted in terms of standard deviations of the prospective measurement error at the LC as described in the TDR. It can be seen that in particular  $h^0 \rightarrow b\bar{b}$  and  $h^0 \rightarrow W^+W^-$  provide good sensitivity to  $m_A$  while the dependence on  $\mu$  is only weak. As a caveat, the values of  $\tan\beta$  as well as the other model parameters are fixed in this study and thus have to be allowed to vary freely in the study or assumed to be known from elsewhere in order to translate the plotted deviations into expected errors on the parameter measurements.

Another study utilizes the ratio  $\mathcal{R} = BR(h^0 \rightarrow b\bar{b})/BR(h^0 \rightarrow \tau^+\tau^-)$  [70]. At tree level, in the MSSM, this ratio is constant since both  $b$  quarks and  $\tau$  leptons are down-type fermions, coupling proportionally to  $\sin\alpha/\cos\beta$  to the  $h^0$ . A precise measurement of this ratio is therefore sensitive to the difference of the radiative corrections to these two decays. In particular at large  $\tan\beta$  these corrections become relevant, allowing to gain sensitivity to the value of  $\tan\beta$  itself if all other SUSY parameters are fixed. The ratio of  $\mathcal{R}^{\text{MSSM}}/\mathcal{R}^{\text{SM}}$  as a function of  $\tan\beta$  is shown in Fig. 20.

### CP violation in the SUSY Higgs Sector

In the MSSM the Higgs potential is invariant under the CP transformation at tree level. However, it is possible to break CP symmetry in the Higgs sector by radiative corrections, especially by contributions from third generation

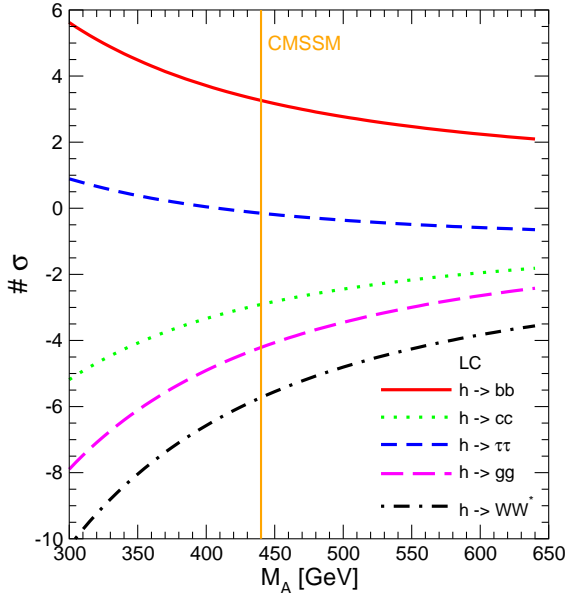


Figure 19: Deviation of decay branching ratios of the lightest CP even Higgs in the constrained MSSM with non-universal Higgs mass (NUHM) (for  $\tan\beta = 10, A_0 = 0, m_{1/2} = 300 \text{ GeV}$  and  $m_0 = 0$ ) from their SM values in terms of standard deviations of the prospective measurement error at the LC as a function of  $\tan\beta$ . The dependence on  $\mu$  is weak (from [69]). The errors are taken from [1].

scalar-quarks [71, 72, 73]. Such a scenario is theoretically attractive since it provides a possible solution to the cosmic baryon asymmetry [74]. In a CP violating scenario the three neutral Higgs bosons,  $H_1, H_2, H_3$ , are mixtures of the CP even and CP odd Higgs fields. Consequently, they all couple to the Z boson and to each other. These couplings may be very different from those of the CP conserving case. In the CP violating scenario the Higgs-strahlung processes  $e^+e^- \rightarrow H_i Z$  ( $i = 1, 2, 3$ ) and pair production processes  $e^+e^- \rightarrow H_i H_j$  ( $i \neq j$ ) may all occur, with widely varying cross-sections.

In a case study, for  $m_{H^\pm} = 200 \text{ GeV}$  and  $\tan\beta = 3$ , the sensitivity of the observable Higgs masses  $m_{H_1}, m_{H_2}$  and of the observed cross-section for  $e^+e^- \rightarrow H_1 H_2 \rightarrow b\bar{b}b\bar{b}$  to the real and imaginary part of the trilinear coupling  $A_t$  has been analyzed. Under the assumption that the other SUSY parameters are known, the complex phase of  $A_t$  may be extracted from these observables [61]. Clearly, further studies are needed in order to extract CP-violating SUSY parameters from the Higgs sector.

## EXTENDED MODELS

### Genuine Dimension-Six Higgs Operators

If a light Higgs boson is discovered at the LHC but no additional particles are seen at the LHC or the LC, it is important to search for small deviations of the Higgs boson

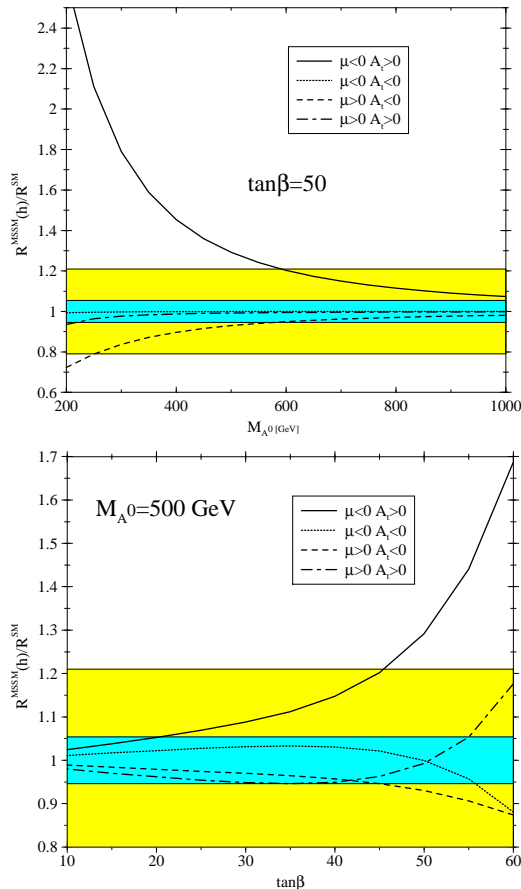


Figure 20: Deviation of the ratio  $\mathcal{R} = BR(h^0 \rightarrow b\bar{b})/BR(h^0 \rightarrow \tau^+\tau^-)$  as a function of  $m_A$  (top) and  $\tan\beta$  (bottom). (from [70]. The inner band represents the expected measurement error taken from [1].

potential from the SM predictions to probe new physics scales. If the reason for such small deviations is beyond-SM physics at large scales  $\Lambda$ , the effective operator approach can be chosen to parameterize the low-energy behavior of such models. Recently, operators of dimension six have been studied, which involve only the Higgs field and which are not severely constrained by precision electro-weak data [75]. These operators are

$$\mathcal{O}_1 = \frac{1}{2}\partial_\mu(\Phi^\dagger\Phi)\partial^\mu(\Phi^\dagger\Phi) \quad \text{and} \quad \mathcal{O}_2 = -\frac{1}{3}(\Phi^\dagger\Phi)^3, \quad (1)$$

which lead to a Lagrangian

$$\mathcal{L}' = \sum_i^2 \frac{a_i}{v^2} \mathcal{O}_i. \quad (2)$$

In [75], it has been shown that the parameter  $a_1$  can be measured to an accuracy of 0.005(0.003) corresponding to a scale  $\Lambda \approx 4$  TeV, from  $1 \text{ ab}^{-1}$  of data at 500 (800) GeV through the measurement of the production cross-sections from Higgs-strahlung and WW/ZZ-fusion for  $m_H = 120$  GeV. The parameter  $a_2$  modifies the form of the Higgs potential and thus the Higgs pair production cross-section.

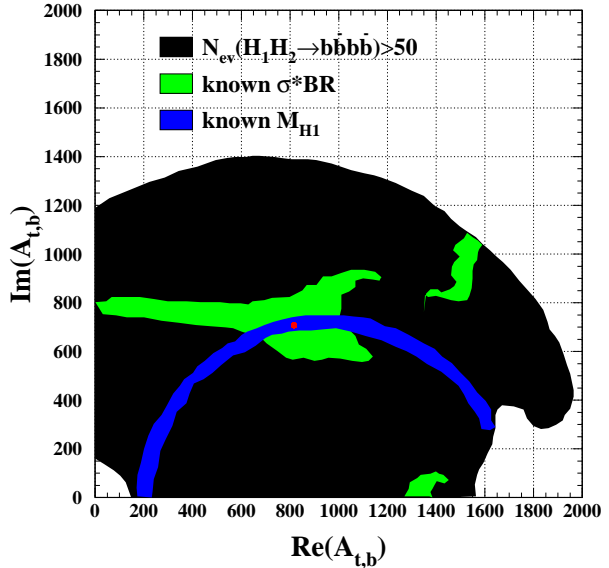


Figure 21: Plane of the real and imaginary part of the trilinear coupling  $A_t$  in a CP violating MSSM scenario. In the black region, the Higgs pair production process  $e^+e^- \rightarrow H_1H_2$  is observable at  $\sqrt{s} = 500$  GeV with  $500 \text{ fb}^{-1}$ . The chosen model point is  $(750, 800)$  GeV for the (real,imaginary) part of  $A_t$ . The dark grey band is the region which is consistent with the measured lightest Higgs mass, the medium grey region is consistent with the measured  $e^+e^- \rightarrow H_1H_2 \rightarrow b\bar{b}b\bar{b}$  rate. The real and imaginary part of  $A_t$  can thus be constrained to the overlapping region. Parameters are  $m_{H^\pm} = 200$  GeV and  $\tan\beta = 3$  (from [61]).

With the same integrated luminosity, for  $m_H = 120$  GeV,  $a_2$  can be measured to  $0.13(0.07)$  at 500 (800) GeV corresponding to a scale  $\Lambda \approx 1$  TeV.

## Two Higgs Doublet Models

The prospects for the exploration of general Two Higgs Doublet Models (2HDM) at a LC have been discussed e.g. in [1]. During the workshop, a 2HDM scenario has been discussed in which the lightest CP-even Higgs boson has absolute values of the tree level couplings to fermions and massive gauge bosons exactly as in the SM and the other Higgs bosons are heavy ( $\mathcal{O}(\text{TeV})$ ) [76]. Within the 2HDM such a scenario can be realized differently from the SM in two ways: (A) the tree level couplings have the same sign as in the SM or (B) either up-type or down-type fermions have opposite sign couplings as in the SM. The only possibility to distinguish such a scenario from the SM is through loop-induced processes, in particular through the loop-induced  $\gamma\gamma h^0$  and  $ggh^0$  couplings. Depending on  $m_h$  the effect can be large enough to be distinguishable from the SM at the LC (and LHC) from Higgs branching ratio measurements or at a photon collider through the  $\gamma\gamma \rightarrow h^0$  process (see Fig. 22).

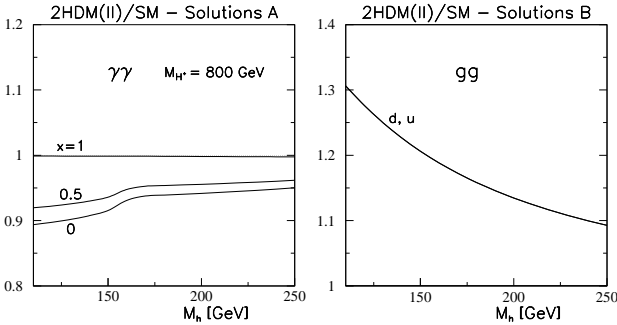


Figure 22: Higgs boson decay widths in the SM-like 2HDM (II) relative to the SM decay widths as functions of  $M_h$ . Left:  $h \rightarrow \gamma\gamma$  decay widths for a 2HDM scenario with all tree-level couplings as in the SM up to an overall sign for  $M_{H^\pm} = 800$  GeV and  $\mu/\sqrt{2} = xM_{H^\pm}$ . Right:  $h \rightarrow gg$ , for a 2HDM scenario with absolute values of tree level couplings as in the SM but opposite relative sign between up-type and down-type fermions (from [76]).

### NMSSM

The addition of a Higgs singlet field defines the Next-to-minimal MSSM (NMSSM). This addition is theoretically motivated mainly since it allows a naturally small  $\mu$  parameter. If the associated Peccei-Quinn symmetry were unbroken, it would lead to a massless CP odd Higgs boson which is ruled out. The LC phenomenology of the model depends on how strong this symmetry is broken. The Higgs spectrum of the NMSSM consists of three CP-even and two CP-odd neutral Higgs bosons and two charged Higgs bosons. The complete LC phenomenology has recently been reviewed in [77]. As an example, the masses of the neutral and charged Higgs bosons and the coupling of the CP-even Higgs bosons to the Z are shown in Fig. 23 as a function of  $m_A$  (defined as the top left parameter of the CP-odd Higgs mixing matrix, see [77]). It can be seen that in a large portion of the parameter space, all three CP-even Higgs bosons would have significant couplings to the Z, thus significant Higgs-strahlung cross-sections at the LC.

### Higgs Bosons and Extra Dimensions

Models which postulate the existence of additional space dimensions in order to explain the hierarchy between the electro-weak and the Planck scale have been discussed extensively in recent years. Their common feature is that the apparent weakness of gravity in our 4-dimensional world is a result of its dilution in the extra dimensions. Two scenarios, that of large extra dimensions (ADD) [78] and that of warped extra dimensions (RS) [79] have been discussed in particular. The 'classic' signatures involve deviations of SM processes like  $e^+e^- \rightarrow ff$  and  $e^+e^- \rightarrow W^+W^-$  from the virtual exchange of towers of (ADD) [80] or single [81] Kaluza-Klein (KK) excitations of gravitons, or their real emission together with SM fermions or gauge bosons [82]. These modes have been studied experimentally e.g. in the

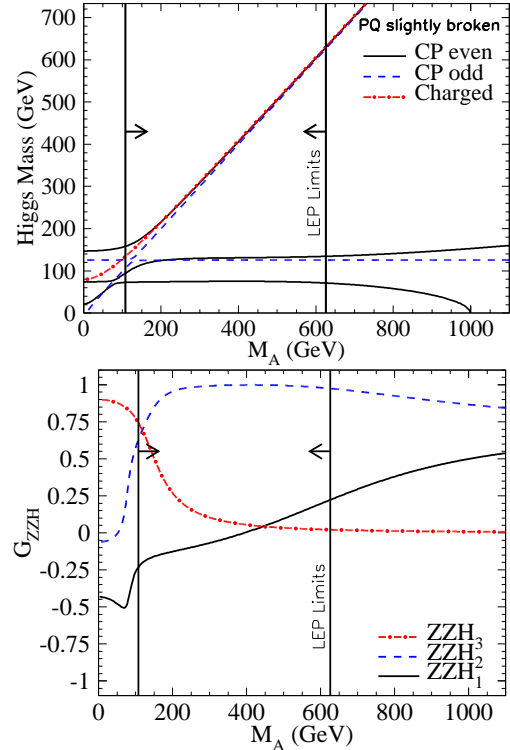


Figure 23: NMSSM Higgs boson properties: masses (upper plot) and couplings of the CP even Higgs bosons to the Z(lower plot) (from [77]) for a scenario with slightly broken Peccei-Quinn symmetry (for  $\lambda = 0.05$ ,  $\kappa = 0.02$ ,  $v_s = 15 v$ ,  $\tan \beta = 3$  and  $A_\kappa = -100$  GeV). The arrows denote the region allowed by LEP searches with 95% confidence.

### TESLA TDR.

More recently, also the impact of extra dimensions on the Higgs boson phenomenology has been studied. In the ADD scenario, two effects have been analyzed:

1. A modification of the quasi-resonant  $W^+W^- \rightarrow H^0$  production process through interference of the SM amplitude with the imaginary part of the graviton/graviscalar KK exchange amplitude [83]. In order to yield a significant modification, a large total Higgs width is needed (i.e. large  $m_H$ ), which implies on the other hand a large center-of-mass energy. While the graviscalar contribution only modifies the normalization of the cross-section (by few percent for  $\sqrt{s} = 1$  TeV,  $m_H = 500$  GeV and 2 extra dimensions at a fundamental Planck scale of 1 TeV), a significant change of the angular distribution is expected from the spin-2 graviton exchange.

2. A modification of the process  $e^+e^- \rightarrow H^0H^0Z$  and the existence of the process  $e^+e^- \rightarrow H^0H^0\gamma$  which is absent at tree level in the SM [84]. For a 1 TeV LC and  $m_H = 120$  GeV, a sizable correction to  $e^+e^- \rightarrow H^0H^0Z$  both in normalization and angular distribution is expected for fundamental Planck scale up to a few TeV. Furthermore, the cross-section for  $e^+e^- \rightarrow H^0H^0\gamma$  exceeds 0.1 fb for a fundamental Planck scale below approximately 2 TeV. In [84],

expected  $5\sigma$  discovery limits on the fundamental Planck scale of 880–1560 (1640–2850) GeV have been derived at  $\sqrt{s} = 500$  (1000) GeV for 6–3 extra dimensions.

In the RS scenario, the influence on the Higgs sector might be much more drastic. Besides the spin-2 KK graviton excitations, graviscalar excitations, called Radions, are predicted [85]. They are predicted to couple to SM particles through the trace of the energy-momentum tensor, i.e. up to the trace anomaly of QCD, very similar to the Higgs boson. The lightest Radion might in fact be lighter than the lightest graviton excitation and thus the discovery channel for the model. Higgs boson and Radion may exhibit kinetic mixing, which leads to a modification of both Higgs boson and Radion properties, in particular their couplings to gauge bosons and fermions. For a review of the Radion phenomenology, see e.g. [86]. The Radion sector is governed by 3 parameters: the strength of the Radion-matter interactions described by an energy scale  $\Lambda_\phi$ , the mass of physical Radion,  $m_\phi$ , and the Radion-Higgs mixing parameter  $\xi$ . In Fig. 24, the effective couplings squared of the Higgs boson and the Radion (relative to those of a SM Higgs boson) are shown for the choice  $\Lambda_\phi = 5$  TeV, and three values of the Radion mass (20, 55, 200 GeV) as a function of  $\xi$ . Large deviations of the Higgs couplings from their SM values are expected if there is large Radion Higgs mixing present. The Radion itself has couplings which are reduced by a factor  $v/\Lambda_\phi$  with respect to those of a SM Higgs in the case of no mixing, which requires high luminosity for direct discovery. The sensitivity of the trilinear Higgs coupling to Radion admixtures has been studied as well in [86].

The LC capability of precisely measuring the Higgs branching ratios  $H^0 \rightarrow b\bar{b}$  and  $H^0 \rightarrow W^+W^-$  has been exploited in [87]. In Fig. 25, the regions where the LC would observe larger than  $2.5\sigma$  deviations of the Higgs branching ratios due to Radion Higgs mixing is shown together with the regions where the LHC can observe the Higgs bosons. In particular the regions in which the LHC might be blind to the Higgs boson are well covered by the LC. A study of the sensitivity of the WW-fusion channel to Radion effects has also been presented at the workshop [88].

## RELATION TO THE LHC

A Higgs boson with SM-like properties will most likely be discovered at the Large Hadron Collider LHC. In recent years, the potential of the LHC to make measurements of Higgs boson properties has been investigated. For a recent summary of the ATLAS studies, see [89]. In most cases the capabilities of a LC are superior to those of the LHC as far as Higgs physics is concerned. In particular, *no model-independent measurements* of Higgs boson couplings are possible at the LHC. However, there are cases where the synergy of both colliders is vital and rewarding. Examples are in the determination of the top Yukawa coupling, in the mass reach for heavy SUSY Higgs bosons, and

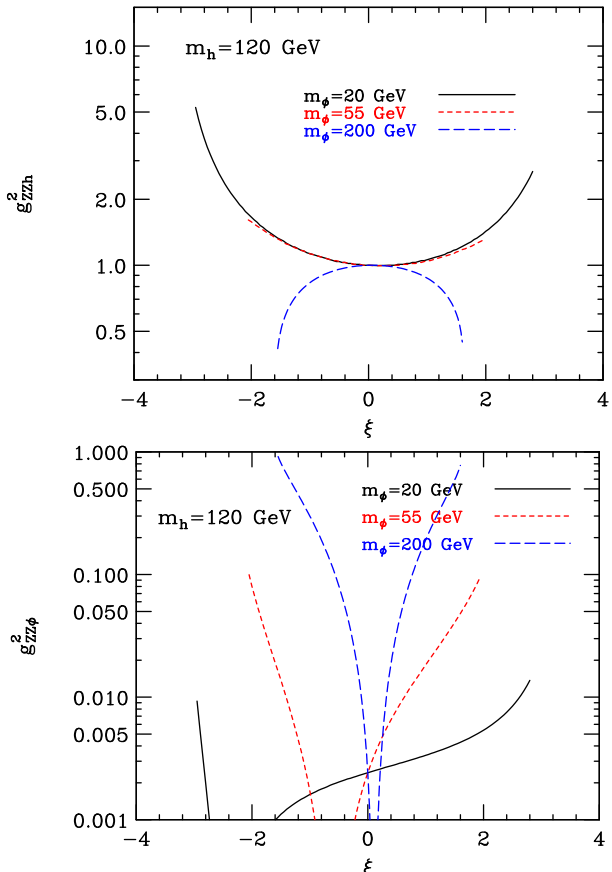


Figure 24: Effective coupling of the Higgs boson (upper) and the Radion (lower) to Z boson (from [86]).

in LHC measurements on third generation squark properties in order to constrain the interpretation of a supersymmetric Higgs sector. These examples are currently been worked out in more detail in a world-wide LHC/LC study group [90].

## SUMMARY AND OUTLOOK

The precision study of Higgs bosons is at the core of the physics program of a future linear collider. In the course of the extended ECFA/DESY study 2001-2003 this physics case has been developed further: the precision of theoretical calculations has been improved, the implication of new theoretical models has been investigated and the experimental studies of the LC sensitivity have been extended and improved.

The studies are vital for the preparation of the worldwide LC project and will be continued both in the three regions America, Asia, and Europe and in worldwide workshops. In Europe, the study will continue in the framework of a new ECFA study. Major goals of this new study are to continue to incorporate new theoretical ideas and to improve the precision of theoretical predictions. On the experimental side, a more detailed study of systematic limitations, impact of machine conditions and in particular dependence of

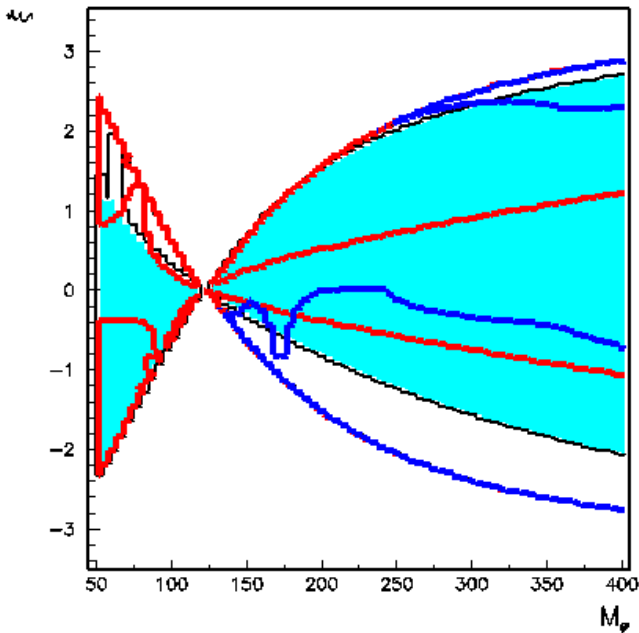


Figure 25: Sensitivity to Radions at LHC and LC: parameter plane of the Radion Higgs mixing angle  $\xi$  and the Radion mass  $M_\phi$  for  $m_H = 120$  GeV. In the shaded regions, the LHC can observe the Higgs boson in the  $gg \rightarrow H^0 \rightarrow \gamma\gamma$  channel with  $30 \text{ fb}^{-1}$  in one experiment. The dark (blue) lines indicate the regions where LHC can observe the Radion in the  $gg \rightarrow \Phi \rightarrow 4\ell$  channel. The grey (red) lines indicate the regions where at the LC a  $> 2.5\sigma$  deviation of the Higgs branching ratio  $\text{BR}(H^0 \rightarrow bb)$  is observable. For more details see [87].

the precision on specific detector properties are of utmost importance.

## ACKNOWLEDGMENTS

I would like to warmly thank all contributors to the Higgs working group for their huge efforts to make the workshop a success. In particular the work of my co-convenors M. Battaglia, A. Djouadi, E. Gross, and B. Kniehl is greatly acknowledged.

## REFERENCES

- [1] ECFA/DESY LC Physics Working Groups, J. A. Aguilar-Saavedra *et al.*, *TESLA Technical Design Report Part III: Physics at an  $e^+e^-$  Linear Collider*, hep-ph/0106315, DESY-2001-011.
- [2] A. de Roeck, these proceedings.
- [3] J. R. Ellis, M. K. Gaillard and D. V. Nanopoulos, Nucl. Phys. B **106** (1976) 292; B. L. Ioffe and V. A. Khoze, Sov. J. Part. Nucl. **9** (1978) 50; B. W. Lee, C. Quigg and H. B. Thacker, Phys. Rev. Lett. **38** (1977) 883.
- [4] D. R. Jones and S. T. Petcov, Phys. Lett. B **84** (1979) 440; R. N. Cahn and S. Dawson, Phys. Lett. B **136** (1984) 196; G. L. Kane, W. W. Repko and W. B. Rolnick, Phys. Lett. B **148** (1984) 367; G. Altarelli, B. Mele and F. Pipolli, Nucl. Phys. B **287** (1987) 205; W. Kilian, M. Kramer and P. M. Zerwas, Phys. Lett. B **373** (1996) 135, hep-ph/9512355.
- [5] B. A. Kniehl, hep-ph/0210176.
- [6] A. Denner, S. Dittmaier, M. Roth, M.M. Weber, *Electroweak radiative corrections to  $e^+e^- \rightarrow \nu\bar{\nu} H$* , Nucl. Phys. B **660** (2003) 289, hep-ph/0302198, LC-TH-2003-007 (2003).
- [7] A. Denner, S. Dittmaier, M. Roth, M.M. Weber, *Electroweak radiative corrections to single Higgs-boson production in  $e^+e^-$  annihilation*, Phys. Lett. B **560** (2003) 196, hep-ph/0301189, LC-TH-2003-008 (2003).  
G. Belanger, F. Boudjema, J. Fujimoto, T. Ishikawa, T. Kaneko, K. Kato and Y. Shimizu, Phys. Lett. B **559** (2003) 252, hep-ph/0212261.  
F. Jegerlehner and O. Tarasov, Nucl. Phys. Proc. Suppl. **116** (2003) 83, hep-ph/0212004.
- [8] A. Djouadi, M. Spira and P. M. Zerwas, Z. Phys. C **70** (1996) 427, hep-ph/9511344.
- [9] A. Djouadi, J. Kalinowski and M. Spira, Comput. Phys. Commun. **108** (1998) 56.
- [10] S. Heinemeyer, W. Hollik and G. Weiglein, *Decay widths of the neutral CP-even MSSM Higgs bosons in the Feynman-diagrammatic approach*, Eur. Phys. J. C **16** (2000) 139, hep-ph/0003022, LC-TH-2001-064.
- [11] T. Sjöstrand, Comp. Phys. Comm. **82** (1994) 74;  
T. Sjöstrand, LU TP 95-20.
- [12] G. Corcella *et al.*, JHEP 01 (2001) 010, hep-ph/0011363;  
hep-ph/0107071, hep-ph/0201201, hep-ph/0210213.  
S. Moretti, *HERWIG: an event generator for  $e^+e^-$  Linear Colliders*, hep-ph/0209209, LC-TOOL-2002-009.
- [13] P. Janot, *Physics at LEP2*, CERN 96-01, Vol.2, 309.
- [14] A. Pukhov *et al.*, hep-ph/9908288.
- [15] W. Kilian, LC-TOOL-2001-039.
- [16] T. Ohl, Comput. Phys. Commun. **101** (1997) 269
- [17] M. Pohl, H.J. Schreiber, *SIMDET - Version 4: A parametric Monte Carlo for a TESLA detector*, LC-DET-2002-005.
- [18] M. Ronan, *Multi-Jet Higgsstrahlung Analysis*, LC-PHSM-2003-048 (2003).
- [19] D. J. Jackson, Nucl. Instrum. Meth. A **388** (1997) 247.
- [20] T. Behnke *et al.*, *BRAHMS: A Monte Carlo for a Detector at a 500/800 GeV Linear Collider*, LC-TOOL-2001-005.
- [21] P. Garcia-Abia and W. Lohmann, Eur. Phys. J. directC **2** (2000) 2.
- [22] S. Dawson, S. Heinemeyer, *The Higgs Boson Production Cross-Section as a Precision Observable?*, Phys. Rev. D **66** (2002) 055002, hep-ph/0203067, LC-TH-2003-005 (2003).
- [23] D. Choudhury, A. Datta and K. Huitu, hep-ph/0302141.
- [24] V. D. Barger, K. m. Cheung, A. Djouadi, B. A. Kniehl and P. M. Zerwas, Phys. Rev. D **49** (1994) 79, hep-ph/9306270.
- [25] S. Y. Choi, D. J. Miller, M. M. Mühlleitner and P. M. Zerwas, *Identifying the Higgs Spin and Parity in Decays to Z Pairs*, Phys. Lett. B **553** (2003) 61, hep-ph/0210077, LC-TH-2003-036 (2003).

[26] M. Kramer, J. H. Kühn, M. L. Stong, and P. M. Zerwas, *Z. Phys. C* **64** (1994) 21, hep-ph/9404280;  
B. Grzadkowski and J. F. Gunion, *Phys. Lett. B* **350** (1995) 218, hep-ph/9501339.

[27] G.R. Bower, T. Pierzchala, Z. Was, M. Worek, *Phys. Lett. B* **543** (2002) 227, hep-ph/0204292;  
M. Worek, *Higgs CP from H/A → tau tau decay*, *Acta Phys. Polon. B* **34** (2003) 4549, hep-ph/0305082, LC-PHSM-2003-050 (2003).

[28] Z. Was and M. Worek, “*Transverse spin effects in H/A → tau+ tau-, tau+- → nu X+-, Monte Carlo approach*”, *Acta Phys. Polon. B* **33** (2002) 1875, hep-ph/0202007], LC-PHSM-2003-049 (2003).

[29] K. Desch, Z. Was and M. Worek, *Measuring the Higgs boson parity at a linear collider using the tau impact parameter and tau → rho nu decay*, *Eur. Phys. J. C* **29** (2003) 491, hep-ph/0302046, LC-PHSM-2003-003 (2003).

[30] A. Imhof, *Measurement of the Higgs boson parity at TESLA*, talk given at the ECFA/DESY workshop on physics and detectors for a future linear collider, Amsterdam, Spring 2003, LC note in preparation.

[31] T. Abe *et al.* [American Linear Collider Working Group Collaboration], *Linear collider physics resource book for Snowmass 2001*, hep-ex/0106055 (part 1), hep-ex/0106056 (part 2), hep-ex/0106057 (part 3), and hep-ex/0106058 (2001).

[32] K. Abe *et al.* [ACFA Linear Collider Working Group Collaboration], *Particle physics experiments at JLC*, hep-ph/0109166.

[33] T. Kuhl, *Higgs branching ratios with SIMDET4+ZVTOP: first results*, talk given at the ECFA/DESY workshop on physics and detectors for a future linear collider, Amsterdam, Spring 2003, LC note in preparation.

[34] M. Battaglia, hep-ph/9910271.

[35] J.-C. Brent, *The direct method to measure the Higgs branching ratios at the future e+ e- linear collider*, LC-PHSM-2002-003 (2002).

[36] M. Battaglia and A. De Roeck, in *Proc. of the APS/DPF/DPB Summer Study on the Future of Particle Physics (Snowmass 2001)* ed. N. Graf, eConf **C010630** (2001) E3066, hep-ph/0111307.

[37] M. Dubinin, H.J. Schreiber, A. Vologdin, *Measurement of the Hzgamma coupling at the future linear e+e- collider*, LC-PHSM-2003-004 (2003).

[38] M. Schumacher, *Investigations of invisible decays of the Higgs boson at a future e+e- linear collider*, LC-PHSM-2003-096.

[39] M. Battaglia, *Rare Higgs Decays: bb and mu mu*, talk given at the ECFA/DESY workshop on physics and detectors for a future linear collider, St. Malo, Spring 2002;  
M. Battaglia, hep-ph/0211461.

[40] N. Meyer, *Measuring Resonance Parameters of Heavy Higgs Bosons at TESLA*, LC-PHSM-2003-066, hep-ph/0308142 (2003).

[41] A. Djouadi, J. Kalinowski and P. M. Zerwas, *Mod. Phys. Lett. A* **7** (1992) 1765.

[42] S. Dittmaier, M. Kramer, Y. Liao, M. Spira and P. M. Zerwas, *Phys. Lett. B* **441** (1998) 383;  
S. Dawson and L. Reina, *Phys. Rev. D* **59** (1999) 054012.

[43] A. Denner, S. Dittmaier, M. Roth and M. M. Weber, hep-ph/0307193; Y. You, W. G. Ma, H. Chen, R. Y. Zhang, S. Yan-Bin and H. S. Hou, *Phys. Lett. B* **571** (2003) 85, hep-ph/0306036;  
G. Belanger *et al.*, *Phys. Lett. B* **571** (2003) 163, hep-ph/0307029.

[44] A. Juste and G. Merino, hep-ph/9910301.

[45] H. Baer, S. Dawson and L. Reina, *Phys. Rev. D* **61** (2000) 013002.

[46] A. Gay, *Top Yukawa coupling*, talk given at the ECFA/DESY workshop on physics and detectors for a future linear collider, Amsterdam, Spring 2003, LC note in preparation.

[47] A. Djouadi, W. Kilian, M. Mühlleitner and P. M. Zerwas, *Eur. Phys. J. C* **10** (1999) 27, hep-ph/9903229.

[48] C. Castanier, P. Gay, P. Lutz and J. Orloff, *Higgs self coupling measurement in e+ e- collisions at center-of-mass energy of 500 GeV*, LC-PHSM-2000-061 (2000).

[49] U. Baur, T. Plehn and D. Rainwater, *Examining the Higgs boson potential at lepton and hadron colliders: A comparative analysis*, hep-ph/0304015.

[50] M. Battaglia, E. Boos and W. M. Yao, in *Proc. of the APS/DPF/DPB Summer Study on the Future of Particle Physics (Snowmass 2001)* ed. N. Graf, eConf **C010630** (2001) E3016, hep-ph/0111276.

[51] G. Degrassi, S. Heinemeyer, W. Hollik, P. Slavich and G. Weiglein, *Towards high-precision predictions for the MSSM Higgs sector*, *Eur. Phys. J. C* **28** (2003) 133, hep-ph/0212020, LC-TH-2002-015.

[52] S. Heinemeyer, W. Hollik and G. Weiglein, *Phys. Rev. D* **58**, 091701 (1998) [hep-ph/9803277]; *Phys. Lett. B* **440**, 296 (1998) [hep-ph/9807423]; *Eur. Phys. J. C* **9**, 343 (1999) [hep-ph/9812472]; M. Carena, H.E. Haber, S. Heinemeyer, W. Hollik, C.E.M. Wagner and G. Weiglein, *Nucl. Phys. B* **580**, 29 (2000) [hep-ph/0001002]; R.-J. Zhang, *Phys. Lett. B* **447**, 89 (1999) [hep-ph/9808299]; J.R. Espinosa and R.-J. Zhang, *JHEP* **003**, 026 (2000) [hep-ph/9912236]; *Nucl. Phys. B* **586**, 3 (2000) [hep-ph/0003246]; J.R. Espinosa and I. Navarro, *Nucl. Phys. B* **615**, 82 (2001) [hep-ph/0104047]; G. Degrassi, P. Slavich and F. Zwirner, *Nucl. Phys. B* **611**, 403 (2001) [hep-ph/0105096]; A. Brignole, G. Degrassi, P. Slavich and F. Zwirner, *Nucl. Phys. B* **631**, 195 (2002) [hep-ph/0112177]; *Nucl. Phys. B* **643**, 79 (2002) [hep-ph/0206101]; Computer programs developed for computing the radiatively-corrected Higgs masses, FeynHiggs and FeynHiggsFast, are described respectively in S. Heinemeyer, W. Hollik and G. Weiglein, *Comput. Phys. Commun.* **124**, 76 (2000) [hep-ph/9812320]; and CERN-TH-2000-055 [hep-ph/0002213].

[53] P.H. Chankowski, S. Pokorski and J. Rosiek, *Nucl. Phys. B* **423** (1994) 437, hep-ph/9303309; *Nucl. Phys. B* **423** (1994) 497;  
V. Driesen and W. Hollik, *Z. Phys. C* **68** (1995), 485, hep-ph/9504335;  
V. Driesen, W. Hollik and J. Rosiek, *Z. Phys. C* **71** (1996) 259, hep-ph/9512441.

[54] S. Heinemeyer, W. Hollik, J. Rosiek and G. Weiglein, *Eur. Phys. J. C* **19** (2001) 535, hep-ph/0102081;  
 S. Heinemeyer and G. Weiglein, *Nucl. Phys. Proc. Suppl.* **89** (2000) 210.

[55] M. Carena, S. Heinemeyer, C. E. Wagner and G. Weiglein, *Eur. Phys. J. C* **26** (2003) 601, hep-ph/0202167.

[56] T. Hahn, S. Heinemeyer and G. Weiglein, *MSSM Higgs-boson production at the linear collider: Dominant corrections to the  $WW$  fusion channel*, *Nucl. Phys. B* **652** (2003) 229, hep-ph/0211204, LC-TH-2002-018.  
 T. Hahn, S. Heinemeyer, G. Weiglein, *Very Heavy MSSM Higgs-Boson Production at the LC*, *Nucl. Phys. Proc. Suppl.* **116** (2003) 336, LC-TH-2002-019 (2002).

[57] H. Eberl, W. Majerotto and V. C. Spanos, *Nucl. Phys. B* **657** (2003) 378, hep-ph/0210038].

[58] J. F. Gunion and H. E. Haber, *Phys. Rev. D* **67** (2003) 075019, hep-ph/0207010.

[59] E. Boos, A. Djouadi, M. Mühlleitner and A. Vologdin, *Phys. Rev. D* **66** (2002) 055004, hep-ph/0205160.

[60] J. F. Gunion *et al.*, *Phys. Rev. D* **38** (1988) 3444; A. Djouadi, J. Kalinowski, P. Ohmann and P. M. Zerwas, *Z. Phys. C* **74** (1997) 93, hep-ph/9605339.

[61] T. Klimkovich, *Experimental study of heavy SuSy Higgs bosons at the LC*, talk given at the ECFA/DESY workshop on physics and detectors for a future linear collider, Amsterdam, Spring 2003, LC note in preparation. A. Raspereza, *CP properties of Higgs bosons and  $H_i H_j \rightarrow b\bar{b}\tau^+\tau^-$  selection*, talk given at the ECFA/DESY workshop on physics and detectors for a future linear collider, Prague, Autumn 2002,  
 A. Raspereza, T. Klimkovich, T. Kuhl, K. Desch, LC note in preparation.

[62] M. Battaglia, A. Ferrari, A. Kiiskinen and T. Maki, in *Proc. of the APS/DPF/DPB Summer Study on the Future of Particle Physics (Snowmass 2001)* ed. N. Graf, *eConf C010630* (2001) E3017, hep-ex/0112015].

[63] S. Kanemura, S. Moretti and K. Odagiri, *JHEP* **0102** (2001) 011, hep-ph/0012030.  
 H. E. Logan and S. f. Su, *Phys. Rev. D* **67** (2003) 017703, hep-ph/0206135.  
 S. Moretti, *Detection of heavy charged Higgs bosons at future Linear Colliders via  $\tau^-\bar{\nu}_\tau H^+$  production*, hep-ph/0209210, LC-TH-2002-010 (2002).  
 O. Brein, hep-ph/0209124.

[64] B. A. Kniehl, F. Madrigal and M. Steinhauser, *Phys. Rev. D* **66** (2002) 054016.

[65] S. Kiyoura, private communication.

[66] J. Gunion, T. Han, J. Jiang, A. Sopczak, *Determining  $\tan(\beta)$  with Neutral and Charged Higgs Bosons*, *Phys. Lett. B* **565** (2003) 42, LC-PHSM-2003-064 (2003).

[67] M. Beccaria, F. M. Renard, S. Trimarchi and C. Verzegnassi, hep-ph/0212167.

[68] A. Dedes, S. Heinemeyer, S. Su and G. Weiglein, hep-ph/0302174, to appear in *Nucl. Phys. B*.

[69] J. Ellis, S. Heinemeyer, K. Olive, G. Weiglein, *Precision Analysis of the Lightest MSSM Higgs Boson at Future Colliders*, *JHEP* **0301** (2003) 006, hep-ph/0211206, LC-TH-2002-013 (2002).

[70] J. Guasch, W. Hollik and S. Peñaranda, *Phys. Lett. B* **515** (2001) 367;  
 J. Guasch, W. Hollik, S. Peñaranda, *Some results on distinction of Higgs boson models*, LC-TH-2003-043 (2003).

[71] A. Pilaftsis and C. E. Wagner, *Nucl. Phys. B* **553** (1999) 3, hep-ph/9902371.

[72] M. Carena, J. R. Ellis, A. Pilaftsis and C. E. Wagner, *Nucl. Phys. B* **586** (2000) 92, hep-ph/0003180.

[73] S. Heinemeyer, *Eur. Phys. J. C* **22** (2001) 521, hep-ph/0108059.  
 M. Frank, S. Heinemeyer, W. Hollik, G. Weiglein, *The Higgs-Boson Masses of the Complex MSSM: A Complete One-Loop Calculation*, hep-ph/0212037, LC-TH-2002-016 (2002).

[74] M. Carena *et al.*, *Nucl. Phys. B* **599** (2001) 158, hep-ph/0011055.

[75] V. Barger, T. Han, P. Langacker, B. McElrath and P. M. Zerwas, *Effects of Genuine Dimension Six Higgs Operators*, *Phys. Rev. D* **67** (2003) 115001, LC-TH-2003-035 (2003).

[76] I. F. Ginzburg, M. Krawczyk, P. Osland, *Two-Higgs-Doublet Models with CP violation*, LC-TH-2003-037 (2003), hep-ph/0211371.

[77] D. J. Miller, R. Nevzorov and P. M. Zerwas, *The Higgs Sector of the Next-to-Minimal Supersymmetric Standard Model*, hep-ph/0304049, LC-TH-2003-034 (2003).

[78] N. Arkani-Hamed, S. Dimopoulos, and G. R. Dvali, *Phys. Lett. B* **429** (1998), 263.

[79] L. Randall and R. Sundrum, *Phys. Rev. Lett.* **83** (1999) 3370, *Phys. Rev. Lett.* **83** (1999) 4690.

[80] J. L. Hewett, *Phys. Rev. Lett.* **82** (1999) 4765.

[81] H. Davoudiasl, J. L. Hewett and T. G. Rizzo, *Phys. Rev. Lett.* **84** (2000) 2080.

[82] G. F. Giudice, R. Rattazzi and J. D. Wells, *Nucl. Phys. B* **544** (1999) 3, hep-ph/9811291.

[83] A. Datta, E. Gabrielli, B. Mele, *Large extra dimension effects in Higgs boson production at linear colliders and Higgs factories*, LC-TH-2003-011 (2003), hep-ph/0303259.

[84] N. G. Deshpande and D. K. Ghosh, *Phys. Rev. D* **67** (2003) 113006, hep-ph/0301272.

[85] G. F. Giudice, R. Rattazzi, and J. D. Wells, *Nucl. Phys. B* **595** (2001) 250.  
 C. Csaki, M. L. Graesser, and G. D. Kribs, *Phys. Rev. D* **63** (2001) 065002.

[86] D. Dominici, B. Grzadkowski, J. F. Gunion and M. Toharia, hep-ph/0206192.

[87] M. Battaglia, S. De Curtis, A. De Roeck, D. Dominici and J. F. Gunion, *On the complementarity of Higgs and radion searches at LHC*, hep-ph/0304245, *Phys. Lett. B* **568** (2003) 92.

[88] A. Datta and K. Huitu, hep-ph/0306241.

[89] M. Dührssen, *'Prospects for measurement of Higgs boson coupling parameters in the mass range from 110 - 190 GeV'*, ATLAS physics note ATL-PHYS-2003-030 (2003).

[90] LHC/LC Study Group, <http://www.ippp.dur.ac.uk/~georg/lhclc/>